

ON THE POSSIBILITY OF SIMPLE PARALLEL COMPUTING OF VORONOI DIAGRAMS AND DELAUNAY GRAPHS

DANIEL REEM

ABSTRACT. The Voronoi diagram is a widely used geometric data structure. The theory of algorithms for computing Euclidean Voronoi diagrams of point sites is rich and useful, with several different and important algorithms. However, this theory has been quite steady during the last few decades in the sense that new algorithms have not entered the game. In addition, most of the known algorithms are sequential in nature and hence cast inherent difficulties on the possibility to compute the diagram in parallel. This paper presents a new and simple algorithm which enables the (combinatorial) computation of the diagram. The algorithm is significantly different from previous ones and some of the involved concepts in it are in the spirit of linear programming and optics. Parallel implementation is naturally supported since each Voronoi cell can be computed independently of the other cells. A new combinatorial structure for representing the cells (and any convex polytope) is described along the way and the computation of the induced Delaunay graph is obtained almost automatically.

1. INTRODUCTION

1.1. Background. In its simplest and widespread form, the Voronoi diagram (the Voronoi tessellation, Dirichlet tessellations) is a certain decomposition of the Euclidean plane (or a region X in the plane) into cells induced by a collection of distinct points p_1, \dots, p_n (called the sites or the generators) and the Euclidean distance. More precisely, the Voronoi cell R_k associated with the site p_k is the set of all the points in X whose distance to p_k is not greater than their distance to the other sites p_j , $j \neq k$. This definition can be easily generalized to other settings, e.g., \mathbb{R}^m , sites having a more general form, various distance functions, etc.

Because they appear in many fields in science and technology and have numerous applications, these diagrams have attracted a lot of attention during the last 4 decades and actually much before [9, 10, 23, 29, 37, 43, 47, 60], especially in the case of 2-dimensional Euclidean Voronoi diagrams of point sites. In particular, many algorithms for computing these diagrams in the above mentioned setting have been published. Among them we mention the naive method [60, pp. 230-233], the divide-and-conquer method [5], [60, pp. 251-257], [72], the incremental method [46], [48], [59], [60, pp. 242-251], the plane sweep method [41], [60, pp. 257-264], [34, Chapter 7], methods based on geometric transforms such as convex hulls [11, 16, 17, 39] (see

Date: April 2, 2015.

2010 Mathematics Subject Classification. 68U05, 68W10, 65D18.

Key words and phrases. Algorithm, combinatorial representation, cone, conic beam, Delaunay graph, parallel computing, ray, subfacet, subcone, vertex, Voronoi diagram.

also [9, 19, 26] and the references therein)) or Delaunay triangulations [22, Chapter 3], [49], [60, pp. 275-80], methods based on lower envelopes [71],[73, p. 241] and methods for very specific configurations [4].

It can be seen that the theory of algorithms for computing 2D Euclidean Voronoi diagrams of point sites is rich and useful, with many different and important algorithms and analyses. However, this theory has been quite steady during the last decades. Some valuable improvements and variations in known algorithms have appeared, but new algorithms have not entered the game.

Another property of this theory is that most of the known algorithms are sequential in nature and they cannot compute each of the cells independently of the other ones. Instead, they consider the diagram as a combinatorial structure and compute it as a whole in a sequential way. This fact casts inherent difficulties on any attempt to implement these algorithms in a parallel computing environment. It is therefore not surprising to see claims such as “Parallelizing algorithms in computational geometry usually is a complicated task since many of the techniques used (incremental insertion or plane sweep, for instance) seem inherently sequential” [9, p. 367] or “It is seldom obvious how to generate parallel algorithms in this area [computational geometry] since popular techniques such as contour tracing, plane sweeping, or gift wrapping involve an explicitly sequential (iterative) approach” [3, p. 293].

Despite what written above, starting from Chow [24] a corresponding theory for parallelizing the computation of Voronoi diagrams has been developed [3, 14, 27, 40, 45, 50, 52, 55, 56, 57, 62, 68] and has been extended to related geometric structures such as the Delaunay triangulation [7, 15, 31, 35, 42, 58, 65, 69, 77, 78, 79]. See [8, 44, 63, 70] and [9, pp. 367-369] for a few surveys. In the works mentioned above the idea is to somehow share the work between the many processing units (under certain assumptions on the computational model), but because of the sequential nature of the involved algorithms, these processing units must cooperate between themselves and cannot work independently. Unfortunately, the above mentioned sequential nature of the involved algorithms complicates the implementation of many of these parallelizing attempts. In addition, a common assumption in the above works is that there are many processing units, e.g., $O(n)$ or $O(n/\log(n))$, where n is the number of sites. This obviously casts difficulties on a practical implementation when the number of sites is much larger than the number of processing units, as usually happens. The result of all of the above is that a significant part of these parallelizing attempts are either theoretical or not widespread. The case of parallelizing attempts in the case of geometric structures related to Voronoi diagrams is somewhat similar: these attempts are either based on the former works or vice versa, or they use somewhat similar techniques or similar assumptions on the computational models and the number of processing units.

The motivation for developing parallel-in-nature algorithms for computational tasks stems from several natural reasons. One important reason is the ability to compute in a fast manner much larger inputs than computed today, in numerous fields, or to perform in a fast way computations which require many iterations, such as centroidal Voronoi diagrams (CVD) [36, 37]. Another reason is that in recent

years most of the computing devices (various types of computers, cell phones, graphic processors, etc.) arrive with several (sometimes with hundreds or even thousands) processing units (cores) which are just waiting for being used. Large networks of such computing devices can be also used for parallel computing tasks.

Taking into account all of the above, it is natural to ask whether there exists an algorithm which can compute each of the Voronoi cells independently of the other ones, and hence can provide a simple way to compute the Voronoi diagram in parallel. To the best of our knowledge, only one such an algorithm has been discussed in the literature, namely the naive one which computes each of the cells by intersecting corresponding halfspaces [60, pp. 230-233]. This (very) veteran algorithm is simple, but it is relatively slow: $O(n^2 \log(n))$ for the whole diagram of n sites in the worst case (assuming 1 processing unit is involved). As claimed in [13], on the average (under the assumption of uniform distribution) its time complexity should behave as $O(n)$. We have not seen any implementation which confirms this, and, as a matter of fact, it seems that in general this algorithm is not used frequently. However, a variation of this naive algorithm for the Delaunay triangulation case has appeared recently in [21], but a careful verification of the data given there shows that when the sites are generated according to the uniform distribution, the implementation behaves in a way which is worse than $O(n)$.

Recently [64], a new algorithm which allows the approximate computation of Voronoi diagrams in a general setting (general sites, general norms, general dimension) was introduced. This algorithm is based on the possibility to represent each cell as a union of rays (line segments), and it approximates the cells by considering a plurality of approximating rays. See Figures 1-2 for an illustration. This algorithm allows the computation of each cell independently of the other ones. However, although in principle the algorithm may compute the combinatorial structure of the cell (e.g., its vertices), this is done in a non-immediate and non-efficient way, since for doing this it needs to somehow detect the corresponding combinatorial components and for achieving this task many rays should be considered and the information obtained from them should be analyzed correctly. What is not clear in advance is to which direction to shoot a ray such that it will hit a vertex exactly. It is therefore natural to ask whether this algorithm can somehow be modified in a such a way that it will allow a simple and efficient computation of the combinatorial structure.

1.2. Contribution of this work. This paper presents and analyzes a new algorithm which enables the combinatorial computation of 2D Euclidean Voronoi diagrams of point sites, where each cell is computed independently of the other ones. In fact, even portions of the same cell can be computed independently of other portions. Parallel implementation is therefore naturally supported. The algorithm is significantly different from previous ones and some of the involved concepts are in the spirit of linear programming and optics. In contrast to many algorithms, the sites can form any configuration (no “general position” assumption to avoid degenerate cases is made). A new combinatorial structure for representing the cells (and any convex polytope) is described along the way, and the computation of the

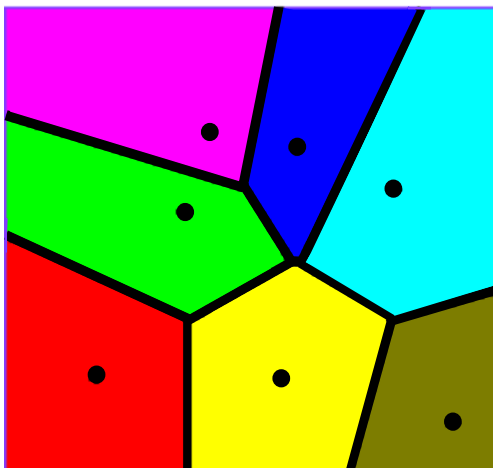


FIGURE 1. A Voronoi diagram of 7 point sites in a square in the Euclidean plane.

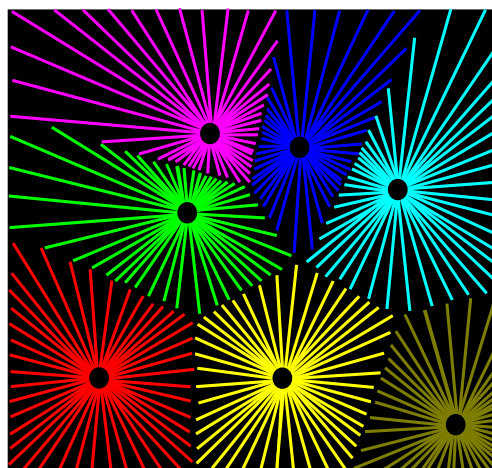


FIGURE 2. Each of the cells of Figure 1 is approximated using 44 rays.

corresponding Delaunay graph (Delaunay triangulation) is obtained almost automatically. The time complexity of the algorithm, as a serial one (one processing unit) for the whole diagram, is bounded above by $O(n^2)$. This upper bound on the time complexity is better than the one of the naive algorithm and it is not known to be tight. The actual behavior is in fact more or less linear when the sites are distributed uniformly. It should be emphasized that this paper is theoretical. Issues related to implementation and experimental results is planned to be discussed elsewhere.

1.3. Paper layout. In Section 2 the notation, terminology and several tools are introduced. In Section 3 a schematic description of the algorithm is given. A detailed description of the algorithm is given in Section 4. A method for finding endpoints in an exact way is described in Section 5. The method of storing the data as well as a discussion on some combinatorial issues are described in Section 6. In Section 7 it is mentioned briefly how the Delaunay graph can be extracted almost automatically from the stored data. Some aspects related to higher dimensions, mainly a new combinatorial representation for the cells (in any dimension), are discussed in Section 8. A discussion on several issues, mainly on the time complexity of the algorithm, is given in Section 9 and in this section the main theorem (Theorem 9.1) is presented. In Section 10 we discuss an improvement of the algorithm which is most efficient in the important case where the sites are distributed independently according to the uniform distribution. The proofs of the main theorem and related claims are given in Section 11. A brief discussion on implementations issues and a possible generalization of the algorithm to non-point sites are given in Section 12.

2. PRELIMINARIES

In this section we present the notation and basic definitions used later, as well as some helpful tools. Our world X is a convex and compact polygon in the Euclidean plane $(\mathbb{R}^2, |\cdot|)$ obtained from the intersection of finitely many half-planes. The induced metric is $d(x, y) = |x - y|$. We denote by $[p, x]$ and $[p, x)$ the closed and half open line segments connecting p and x , i.e., the sets $\{p + t(x - p) : t \in [0, 1]\}$ and $\{p + t(x - p) : t \in [0, 1)\}$ respectively. The inner product between the vectors $x = (x_1, x_2)$ and $y = (y_1, y_2)$ is $\langle x, y \rangle = \sum_{i=1}^2 x_i y_i$. A nonnegative linear cone emanating from a point p and generated by the vectors t_1, t_2 is the set $\{p + \sum_{i=1}^2 \lambda_i t_i : \lambda_i \geq 0, i = 1, 2\}$. Lines are denoted by L, M , etc. A facet of a polygon located on a corresponding line L is denoted by \tilde{L} . In dimension 2 a facet of the cell is just an edge and we alternatively use the names “edge”, “side”, or “facet” for describing this notion. The sites are distinct points denoted by $p_k, k \in K = \{1, \dots, n\}$.

Definition 2.1. *The Voronoi diagram of the tuple of point sites $(p_k)_{k=1}^n$ contained in the region X is the tuple $(R_k)_{k=1}^n$ of subsets $R_k \subseteq X$ where, for each $k \in K = \{1, \dots, n\}$,*

$$R_k = \{x \in X : d(x, p_k) \leq d(x, p_j) \quad \forall j \in K, j \neq k\}.$$

In other words, the Voronoi cell R_k associated with the site p_k is the set of all $x \in X$ whose distance to p_k is not greater than their distance to the other sites p_j .

The definition of the Voronoi diagram is analytic. However, it can be easily seen that each cell R_k is the intersection of the world X with halfplanes: the halfplanes $\{x \in \mathbb{R}^2 : d(x, p_k) \leq d(x, p_j), j \neq k\}$. Thus each cell is a closed and convex set which can be represented using its combinatorial structure, namely its vertices and sides. Because of this property the traditional approach to Voronoi diagrams is combinatorial.

In a recent work [64], a different representation of the cells was introduced, suggesting to consider each of the cells as a union of rays (lines segments). See Figure 2. This representation is related to, but different from, the fact that the Voronoi cells are star-shaped. The theory of Voronoi diagrams in general and of algorithms for computing Voronoi diagrams in particular, is very diverse, with plenty of interesting and important facts and ideas. In particular, the star-shaped property of the cells is a well-known fact. However, to the best of our knowledge, and this is said after an extensive search that we have made in the literature (for many years) and after conversations with, or in front of, many experts, in various scientific and technological domains, there has been no attempt to use any kind of ray-shooting techniques to compute (possibly approximately) the Voronoi cells.

Theorem 2.2. *The Voronoi cell R_k of a site $p = p_k$ is a union of rays emanating from p in various directions. More precisely, denote $A = \bigcup_{j \neq k} \{p_j\}$. Given a unit vector θ , let*

$$T(\theta, p) = \sup\{t \in [0, \infty) : p + t\theta \in X \text{ and } d(p + t\theta, p) \leq d(p + t\theta, A)\}. \quad (2.1)$$

The point $p + T(\theta, p)\theta$ is the endpoint corresponding to the ray emanating from p in the direction of θ . Then

$$R_k = \bigcup_{|\theta|=1} [p, p + T(\theta, p)\theta].$$

This representation actually holds (after simple modifications) in a more general setting (any norm, any dimension, sites of a general form, etc.) and it shows that by “shooting” enough rays one can obtain a fairly good approximation of the cells (see Figures 1-2). It will be shown later how the idea of shooting rays can be used for obtaining the combinatorial structure of the cells.

3. A SCHEMATIC DESCRIPTION OF THE ALGORITHM

This section gives a schematic description of the algorithm. The method is based on the fact that the cell of some point site $p = p_k$ is a convex polygon whose boundary consists of vertices and edges. Some of the involved concepts are in the spirit of optics and linear programming. We first provide a high-level description and later a detailed one. Recall again that for a unit vector θ , the point $p + T(\theta, p)\theta$ is the endpoint corresponding to the ray emanating from p in the direction of θ (see Figure 2). From now on we assume that all the sites are distinct, known in advance, and no site is located on the boundary of the world X .

Method 3.1. *A high level description:*

- **Input:** A site p ;
 - **Output:** The (combinatorial) Voronoi cell of p ;
- (1) Think of p as a light source;
 - (2) emanate a (linear) conic beam of light from p using a simplex;
 - (3) detect iteratively (by possibly dividing the cone to subcones) all possible vertices (and additional related combinatorial information) inside this beam using corresponding endpoints and an associated system of equations;
 - (4) continue the process with other beams until the whole space around p is covered;

The actual generation and handling of the (sub)cones is done using a simplex (triangle) located around p . See Figure 3. The boundary of this simplex is initially composed of one-dimensional facets, and later these facets are composed of subfacets, when we narrow the search to subcones (sub-beams). Each such a subfacet induces a cone: the cone generated by the rays which pass via the corners of the subfacet. Each such a corner induces a unit vector (denoted by θ) which points in its direction (from p). Once the corresponding unit vector is known, then so is the ray in its direction. We use a simple data structure called *FacetQueue* which maintains a dynamic list of subfacets so that the whole implementation is based on loops instead of recursive programming. Initially there are 3 subfacets (the ones of the simplex) and later subfacets are added or omitted.

The system of equations mentioned above (Step (3)) is

$$B\lambda = H, \tag{3.1}$$

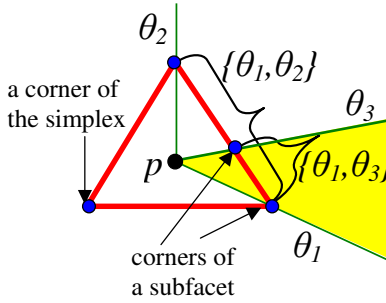


FIGURE 3. The simplex, some of its subfacets, and the conic beam emanating from p and corresponding to the subfacet $\{\theta_1, \theta_3\}$.

where the vector of unknowns is $\lambda = (\lambda_1, \lambda_2)$, B is the 2 by 2 matrix with entries $B_{ij} = \langle N_i, T_j \rangle$ and H is a 2-dimensional vector with entries $H_i = \langle N_i, T_i \rangle, i, j \in \{1, 2\}$. The notation $T_i = T(\theta_i, p)\theta_i$ means the vector in direction θ_i whose length is the distance from p to the endpoint $p + T_i$. The 2-dimensional vector N_i is a normal to the line $L_i = \{x : \langle N_i, x \rangle = c_i = \langle N_i, p + T_i \rangle\}$ on which the endpoint $p + T_i$ is located. Solving the linear 2 by 2 system of equations (3.1) is a simple and well-known task, either in an exact way (exact arithmetic) or using floating point arithmetic.

Equation (3.1) has a simple geometric meaning: the point $u = p + \sum_{i=1}^2 \lambda_i T_i$ is in the intersection of the lines L_1, L_2 if and only if λ solves (3.1). If we want to restrict ourselves to the cone generated by the corresponding rays, then we consider only the nonnegative solutions of (3.1), i.e., $\lambda_i \geq 0$ for all $i = 1, 2$. If equation (3.1) has a unique nonnegative solution λ , then this means that u is a point in the cone which is a candidate to be a vertex of the cell, since it may be (but is not necessary) in the intersection of the corresponding 2 different facets located on the lines L_i . If, in addition, u is known to be in the cell, then it is indeed a vertex.

Remark 3.2. To the best of our knowledge, Method 3.1 above (and its detailed form, Algorithm 1 below) is new. There are many differences between it and existing algorithms, e.g., its ability to compute each cell or parts of a cell independently of the other cells, its use of rays and cones, the fact that it first detects facets of a cell and later vertices, etc.

Recently we were informed that there are papers in the computational geometry literature (e.g., [6, 28]), which, although not considering Voronoi diagrams, they still use rays in order to detect boundary of geometric objects. This is done via a mechanism called “geometric probing”. At first glance one may think that these papers do have some relation to our method. However, it can be verified quickly that the settings and methods described in these papers are significantly different from the method described in our one and their actual relation to our paper is quite

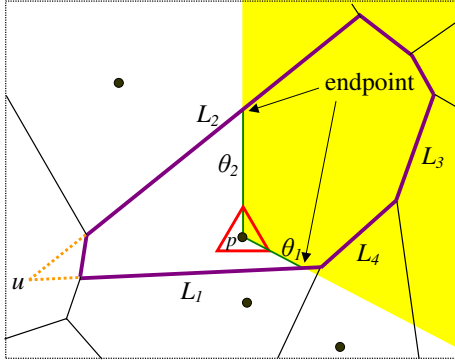


FIGURE 4. Illustration of the algorithm. The cone generated by the subfacet $\{\theta_1, \theta_2\}$ is shown. The intersection between L_1 and L_2 is a point outside the cone and hence the cone is divided. The next two subfacets are $\{\theta_1, \theta_3\}$, $\{\theta_2, \theta_3\}$.

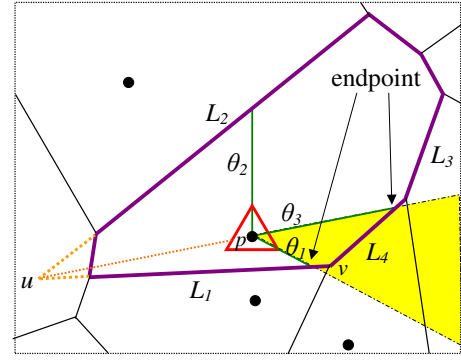


FIGURE 5. Now the cone generated by the subfacet $\{\theta_1, \theta_3\}$ is shown. Since $v = L_1 \cap L_4$ is a point in the cone and the cell it is a vertex and no further dividing of this cone is needed.

weak. (Besides, our paper has not been inspired by these papers, since, as implied above, we were not aware of them until recently.)

For instance, the probing done in [6, Fig. 1, page 162] is performed by a robot, which goes, from the outside, around the boundary of the given 2D object, and use its arms (or an optical device) in order to touch (probe) the boundary. By this way it obtains a collection of points from the boundary (denoted by P). Denote by L the collection of rays emanating from the various locations of the robot when it goes around the object and probes the geometric object. Then (page 163): “the aim is to join the points of P without intersecting the rays of L , in order to find a polygonal approximation of the object boundary”. Similar things can be said regarding [28]. In comparison, in our method all the rays emanate from a unique point (the site), this point is located inside the geometric object (the Voronoi cell), the computation of the endpoints is not trivial (the boundary of the object is not known, in contrast to the geometric probing case), and the goal is not to connect the endpoints in order to obtain a polygonal approximation of the boundary of the Voronoi cell, but rather to use these endpoints in order to detect facets (edges) and later vertices of the cell.

4. A DETAILED DESCRIPTION OF THE ALGORITHM

This section presents a more detailed description of Method 3.1, including a pseudocode. See Figures 4-5 for an illustration. An additional related illustration is given in Figure 11. The description below and the one given in Algorithm 1 use the same notation.

First, we create the 3 unit vectors θ_i corresponding to a simplex around the point p . After choosing a simplex subfacet, shooting the two rays in the direction of θ_i , $i = 1, 2$, finding the endpoints $p + T_i$ (using, e.g., Method 5.1 in Section 5; here

Algorithm 1: The algorithm: a detailed pseudocode

input : A site p whose Voronoi cell is to be computed, the other sites
output: The vertices and edges of the cell, other information

- 1 Create the simplex unit vectors;
- 2 Create the simplex facets and enter them into *FacetQueue*;
- 3 **while** *FacetQueue* is nonempty **do**
- 4 Consider the highest (first) subfacet in *FacetQueue*;
- 5 Denote it by $\{\theta_1, \theta_2\}$;
- 6 Compute the endpoints $p + T_i$, $i = 1, 2$ (see Method 5.1 and Method 10.2);
- 7 Find their neighbor sites a_i , $i = 1, 2$;
- 8 Compute the bisecting line L_i between p and a_i , $i = 1, 2$;
- 9 If no such a site a_i exists, then $p + T_i$, is on the boundary of the world. Call the corresponding boundary line L_i ;
- 10 Consider the system of equations (3.1)
- 11 **if** $\det(B) = 0$ **then** // no solution or ∞ many
- 12 | **if** $L_1 = L_2$ **then** // no vertices here
- 13 | | continue;
- 14 | **else** // parallel lines
- 15 | | $\theta_3 = \phi$ where ϕ is the direction vector of the lines;
- 16 | | If the ray in the direction of ϕ is not in the cone, then $\theta_3 = -\phi$;
- 17 | | Insert the subfacets $\{\theta_1, \theta_3\}$, $\{\theta_2, \theta_3\}$ into *FacetQueue*;
- 18 | **else** // $\det(B) \neq 0$, unique solution $\lambda = (\lambda_1, \lambda_2)$
- 19 | | $u = p + \lambda_1 T_1 + \lambda_2 T_2$;
- 20 | | **if** λ is nonnegative **then** // we're in the cone
- 21 | | | **if** u is inside the cell **then**
- 22 | | | | Store u , L_1, L_2 (and/or neighbor sites;) // u is a vertex
- 23 | | | | **else** // u is outside the cell
- 24 | | | | | $\theta_3 = (u - p)/|u - p|$;
- 25 | | | | | Insert $\{\theta_1, \theta_3\}$, $\{\theta_2, \theta_3\}$ into *FacetQueue*;
- 26 | | | | **else** // u isn't in the cone
- 27 | | | | | $\theta_3 = (p - u)/|p - u|$;
- 28 | | | | | Insert $\{\theta_1, \theta_3\}$, $\{\theta_2, \theta_3\}$ into *FacetQueue*;
- 29 | Remove $\{\theta_1, \theta_2\}$ from *FacetQueue*;

$T_i = T(\theta_i, p)\theta_i$) and finding the corresponding bisecting lines L_i , we want to use this information for finding all of the possible vertices in the cone generated by the rays. By using equation (3.1) we find the type of intersection between the lines L_1, L_2 . This intersection is either the empty set, a point, or a line.

If (3.1) has no solution of any kind (including solutions which are not non-negative), then the lines L_1 and L_2 are parallel. This is a rare event but it must be taken into account. In this case L_1 and L_2 have the same direction vector ϕ , i.e., $L_i = \{q_i + \phi t : t \in \mathbb{R}\}$ for some $q_i \in \mathbb{R}^2$, $i = 1, 2$ and some unit vector ϕ . We check if the ray emanating from p in the direction of ϕ is in the cone (happens if and only if the solution (α_1, α_2) to the linear equation $\phi = \alpha_1\theta_1 + \alpha_2\theta_2$ is nonnegative). If

yes, then we shoot a ray in the direction of $\theta_3 := \phi$. Otherwise, we shoot the ray in the direction of $\theta_3 = -\phi$. This ray will be contained in the cone and will hit a facet of the cell not located on the lines L_1 and L_2 (the facet may be located on the boundary of the bounded world X). We divide the current simplex subfacet using θ_3 and continue the process.

If $L_1 = L_2$, then both endpoints are located on the same line. This corresponds to the case where (3.1) has infinitely many solutions. In this case there is no vertex in the corresponding cone (perhaps one of the endpoints $p + T_i$ is a vertex, but this vertex will be found later using the neighbor subfacet: see Lemma 11.14). Hence we can finish with the current subfacet and go to the other ones. Such a case is implicit in Figure 4 when the rays are shot in the directions of the first and third corners of the simplex and hit L_1 .

If (3.1) has a unique solution $\lambda = (\lambda_1, \lambda_2)$, then either it is not nonnegative, i.e., the point $u = p + \sum_{i=1}^2 \lambda_i T_i$ is not in the cone, or λ is nonnegative, i.e., u is in the cone. In the first case the ray emanating from p in the direction of $\theta_3 := (p-u)/|p-u|$ will hit an edge of the cell contained in the cone but not located on L_1 or L_2 . Such a case is described in Figure 4 when considering the subfacet $\{\theta_1, \theta_2\}$. We divide the current simplex subfacet using θ_3 and continue the process. In the second case u is in the cone, but we should check whether u is in the cell (can be checked, for instance, by distance comparisons). If u is in the cell (a case corresponding to the case of the subfacet $\{\theta_1, \theta_3\}$ in Figure 5, where $u = v$ there), then it is a vertex and we store it (together with other data: see Section 6). We have finished with the subfacet and can go to the other ones. Otherwise u is not a vertex, and we actually found a new edge of the cell corresponding to the ray in the direction of $\theta_3 := (u-p)/|u-p|$ (implicit in Figure 4 when considering the subfacet $\{\theta_2, \theta_3\}$, i.e., the rays are shot in the directions of the second and third corners of the simplex; in this case u is the intersection of L_1 and L_2). We divide the subfacet using θ_3 and continue the process.

We avoid a recursive implementation of the algorithm and base it on loops using a simple data structure called *FacetQueue*. This list stores temporarily the simplex subfacets that are handled during the process (each subfacet is represented by a set of two unit vectors, which correspond to its corners). The algorithm runs until *FacetQueue* is empty. The initial list contains the sides (facets) of the simplex $\{\psi_1, \psi_2\}$, $\{\psi_2, \psi_3\}$, $\{\psi_1, \psi_3\}$, where we can take $\psi_1 = (\sqrt{3}/2, -1/2)$, $\psi_2 = (0, 1)$, $\psi_3 = (-\sqrt{3}/2, -1/2)$.

In this connection, it should be emphasized that the simplex is used for handling the progress of the algorithm (using *FacetQueue*), but the corresponding unit vectors in the direction of the subfacets' corners are not necessarily on the same line as the one on which the simplex subfacet is located. Despite this, it is convenient to represent a simplex subfacet by its associated unit vectors.

5. FINDING THE ENDPOINTS EXACTLY

In order to apply Method 3.1, we should be able to find the endpoint $p + T(\theta_i, p)\theta_i$ emanating from the site p in the direction of θ_i (see (2.1) and line 6 in Algorithm

1). One possible method is to use the method described in [64], but the problem is that the endpoint found by this method is given up to some error parameter, and unless this parameter is very small (which, in this specific case, implies slower computations), this may cause an accumulating error later when finding the vertices, due to numerical errors in the expressions in (3.1).

In what follows we will describe a new method for finding the endpoint in a given direction θ exactly. Of course, when using floating point arithmetic errors appear, but they are much smaller than the ones described above. See Figure 6 for an illustration.

Method 5.1.

- **Input:** A site p and a unit vector θ ;
 - **Output:** the endpoint $p + T(\theta, p)\theta$.
- (1) Shoot a ray from p in the direction of θ and stop it at a point y which is either in the region X but outside the cell of p (see Method 10.2 below), or it is the intersection of the ray with the boundary of the region (see Remark 5.2 below). If y is chosen to be outside the cell, then go to Step (4). Otherwise, let L be the boundary line on which y is located;
 - (2) check whether y is in the cell, e.g., by comparing $d(y, p)$ to $d(y, a)$ for any other site a , possibly with enhancements which allow to reduce the number of distance comparisons;
 - (3) if y is in the cell, then y is the endpoint and L is the bisecting line. The calculation along the ray is complete;
 - (4) otherwise, $d(y, a) < d(y, p)$ for some site a . Let $CloseNeighbor := a$;
 - (5) find the point of intersection (call it u) between the given ray and the bisecting line L between p and $CloseNeighbor$. This intersection is always nonempty. The line L is easily found because it is vertical to the vector $p - CloseNeighbor$ and passes via the point $(p + CloseNeighbor)/2$;
 - (6) let $y := u$; go to Step (2).

Remark 5.2. Below we discuss two simple methods for computing the intersection between the ray Γ_θ emanating from p in the direction of θ and the boundary of X . This ray can be represented as $\Gamma_\theta = \{p + t\theta : t \geq 0\}$.

One method is an approximate one, in the spirit of [64]. We fix a small positive parameter ϵ , select a point $y \in \Gamma_\theta$ which is known to be outside X (just a point very far from p), denote $x := p$, select the midpoint $z := 0.5(x + y)$ between x and y , and check if z is in X . If yes, then we let $x := z$, otherwise we let $y := z$. This bisecting process continues until the length of the segment $[x, y]$ is smaller than ϵ . The advantage of this method is that it is simple and general (works for any type of boundary of X , not necessarily polygonal), but it can be somewhat slow and it does not lead to an exact output.

The second method is exact and is restricted to the case where we assume that X is a compact polygon obtained from the intersection of finitely many (say m) half-planes H_j (the basic assumption in this paper). In this case the boundary of X is a finite union $\cup_{j=1}^m I_j$ of line segments (edges) I_j . We can write $H_j = \{x =$

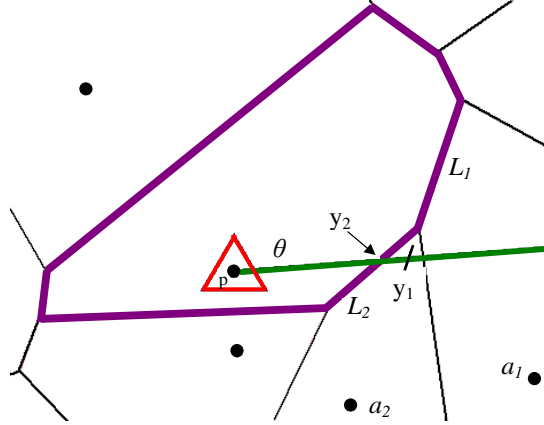


FIGURE 6. Illustration of Method 5.1 for some ray. At the first displayed iteration *CloseNeighbor* is a_1 . The intersection between the corresponding line L_1 and the ray is $y = y_1$. At the next stage *CloseNeighbor* is a_2 and $y = y_2$. The process terminates since y_2 is in the cell of p , i.e., it is the endpoint.

$(x_1, x_2) \in \mathbb{R}^2 : \langle N_j, x \rangle \leq c_j$ where $N_j \in \mathbb{R}^2$ is the normal to the boundary line $L_j = \{x = (x_1, x_2) \in \mathbb{R}^2 : \langle N_j, x \rangle = c_j\}$ of H_j and $c_j \in \mathbb{R}$ is a constant.

The considered ray intersects L_j if and only if there exists $t_j > 0$ such that $p + t_j\theta \in L_j$, i.e., $\langle N_j, p \rangle + t_j\langle N_j, \theta \rangle = c_j$ (the case $t_j = 0$ is impossible since p is assumed to be in the interior of X). Therefore, either $\langle N_j, \theta \rangle = 0$ and then the ray is parallel to L_j and the intersection is empty, or

$$t_j = \frac{c_j - \langle N_j, p \rangle}{\langle N_j, \theta \rangle} \quad (5.1)$$

where it should be verified that $t_j > 0$.

Summarizing the above, we go over all the boundary edges I_j and check whether t_j defined by (5.1) is well defined (i.e., $\langle N_j, \theta \rangle \neq 0$) and is positive. Among those t_j which satisfy these conditions we verify that $p + t_j\theta \in X$, i.e., $p + t_j\theta \in H_k$ for all $k \in \{1, \dots, m\}$. Analytically, we should verify that for each such j we have

$$t_j\langle N_k, \theta \rangle \leq c_k - \langle N_k, p \rangle, \quad \forall k \in \{1, \dots, m\}. \quad (5.2)$$

Any t_j which satisfies (5.2) leads to the point of intersection between the ray Γ_θ and the boundary of X (usually there will be a unique t_j , unless the ray passes through a vertex of X ; the existence of at least one t_j is a consequence of the intermediate value theorem: see the proof of Lemma 11.1). As a final remark, we note that in

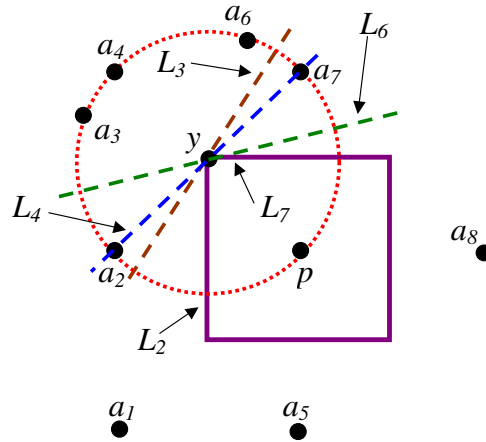


FIGURE 7. Illustration of Remark 5.4. Here y is a vertex of the cell of p (the square), $EquiDistList = \{a_2, a_3, a_4, a_6, a_7\}$, and L_i are the bisectors between p and a_i for $i \in \{2, 3, 4, 6, 7\}$. The smallest distances $d(p, a_i)$, $a_i \in EquiDistList$ are $d(p, a_2)$, $d(p, a_7)$ and indeed L_2, L_7 contain edges of the cell of p .

(5.2) we do not really need to go over all $k \in \{1, \dots, m\}$ but rather on those $k \neq j$ for which t_k defined by (5.1) is well defined and positive.

Remark 5.3. Method 5.1 is correct, as shown below. First, the method terminates after finitely many steps because there are finitely many sites. The point u in Step (5) is well defined because y is in the halfspace of $CloseNeighbor$ and hence the considered ray intersects the boundary L of this halfspace. The point y is outputted in Step (3) and by the description of this step y is in the cell. Since y is on a bisecting line between p and another site, and since y is in the cell, this means that y must be an endpoint (see (2.1); here $A = \cup_{j \neq k} \{p_j\}$ and $T(\theta, p) = |y - p|$).

Remark 5.4. When finding the endpoint y , one can also find all of its neighbor sites since in the last time Step (2) is performed, one can easily find all the sites a satisfying $d(a, y) = d(p, y)$ simply by storing any site a satisfying this equality. Call the corresponding list $EquiDistList$. Each $a \in EquiDistList$ induces a corresponding bisecting line L between p and a . In the rare event where y coincides with a vertex of the cell, there may be $a \in EquiDistList$ whose bisector L may not contain a facet of the cell but rather it intersects the cell only at the vertex y (this can happen only when $EquiDistList$ has at least 3 different elements, i.e., at least 3 distinct sites located on a circle around y , and hence this cannot happen when the sites are in general position). This is a problem, since we want to make sure that

when we make operations with the endpoint, we use a line L on which this endpoint is located and on which an edge of the cell is located.

In order to overcome the problem, we need to determine the sites $a \in EquiDistList$ that induce bisectors containing an edge of the cell, and then to consider these sites and their associated lines for later operations. This can be achieved by sorting in increasing order all the angles $\angle pya$, $a \in EquiDistList$, or, equivalently, the distances $d(a, p)$, $a \in EquiDistList$ (the equivalence is because p and all the sites $a \in EquiDistList$ are on a circle whose center is y). The sites corresponding to the two smallest values are the ones which induce a desired bisector, and we can associate with y any one of these sites and their corresponding bisectors. See Figure 7.

6. STORING THE DATA

Given a point site $p = p_k$, when a vertex u belonging to the cell of p is found, one stores the following parameters: its coordinates, the lines from which it was obtained (i.e., u belongs exactly to the corresponding facets located on these lines), and the index k . For storing a line L it is convenient to store the index of its associated neighbor site, namely the index (simply a number or a label) of the site which induces it (denoted by *CloseNeighbor* in Method 5.1). If it is a boundary line, then it has a unique index number which is stored and from this index one can retrieve the parameters (the normal and the constant) defining the line. Alternatively, these parameters can be stored directly. For some purposes it may be useful to store also some endpoints.

A convenient data structure for the storage is a one dimensional array, indexed by k , in which the vertices (represented, as explained above, by coordinates and associated neighbor sites) and any additional information, such as endpoints, are stored. Although the vertices are not stored according to a certain order, it is quite easy to sort them later in clockwise or counterclockwise order by the method of search, e.g., by labeling the rays with corresponding values.

7. COMPUTING THE DELAUNAY GRAPH (DELAUNAY TRIANGULATION)

As is widely known, the Delaunay graph is an important geometric structure which is closely related to the Voronoi diagram and by itself has many applications [9, 22, 34, 60]. By definition, it consists of vertices and edges. The vertices are the (point) sites. There is an edge between two sites if their Voronoi cells are neighbors (via a facet). See Figure 8 for an illustration.

The computation of the restriction of the Delaunay graph to the given bounded world X , from the stored data structure of the Voronoi diagram, is simple and done almost automatically: one chooses a given site, goes over the data structure and finds all the different neighbor sites of a given site. The procedure is repeated for each site and can be easily implemented in parallel.

Note that here everything is restricted to the given bounded world X . Rarely it may happen that two sites whose cells are neighbors in the whole plane are not neighbors in X . This can happen only with cells which intersect the boundary of X . For overcoming this problem (if one considers this as a problem) one can simply

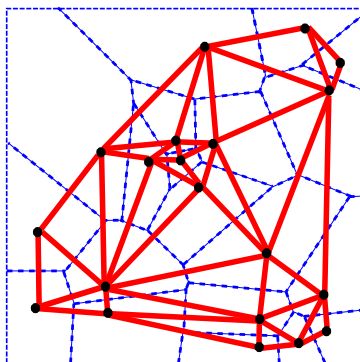


FIGURE 8. The Delaunay graph of 20 sites, restricted to a square (thick lines), together with the Voronoi cells of the sites (thin lines).

take X to be large enough or can perform a separate check for the above boundary cells.

8. A NEW COMBINATORIAL REPRESENTATION FOR THE CELLS

As explained in Section 6, each vertex is stored by saving its coordinates and the facets (actually the corresponding neighbor sites which induce these facets) which intersect at the vertex. This section extends this idea to higher dimensions and presents a new combinatorial representation for the Voronoi cells (and actually any convex polytope) in this setting.

In dimension $m = 2$ a vertex u is always obtained from the intersection of 2 lines. In dimension $m \geq 3$ a vertex is usually obtained from exactly m hyperplanes, but in principle it can be obtained from S hyperplanes, $S > m$. We call the set $\{L_{i_1}, \dots, L_{i_S}\}$ of all the hyperplanes from which u was obtained the combinatorial representation of u .

As the examples below show (see also Section 7), once the above combinatorial representation is known and stored, we can obtain other combinatorial information related to the cell, say the neighbors of a given vertex, the ℓ -dimensional faces of some cell, and so on, and hence we do not need to store these types of information separately. This is in contrast to familiar methods for representing the combinatorial information in which one has to find and store all the ℓ -dimensional faces, $\ell = 0, 1, \dots, m - 1$ of the cell. Since the combinatorial complexity of the cell (the number of multi-dimensional faces) can grow exponentially with the dimension [9, 53], our method may reduce the required space needed for the storage (at least by improving some constants). The price is however that for retrieving some data certain search operations will have to be done on the stored information. There is another difference between our method and other ones. In other methods one starts with the vertices as the initial (atomic) ingredients, and from them one constructs higher dimensional faces. For instance, an edge is represented by the two vertices

which form its corners. However, in our method we start with the highest dimensional faces (located on hyperplanes) and from them we construct the vertices and the other multi-dimensional faces. As a matter of fact, our method of storage can be used to represent any multi-dimensional convex polytope, and even a class of nonconvex or abstract ones.

Example 8.1. The possible ℓ -dimensional faces, $\ell = 0, 1, \dots, m-1$, can be found by observing that any such a face is the intersection of hyperplanes. Indeed, the $(m-1)$ -dimensional faces are all the hyperplanes L_i which appear in the representation of the vertices. For finding the $(m-2)$ -dimensional faces we fix an hyperplane L_i and look at all the vertices u having L_i in their combinatorial representation. In the representation of any such a vertex u appear other hyperplanes L_j , and $L_i \cap L_j$ is an $(m-2)$ -dimensional face. By going over all the possible hyperplanes of u , all the possible u , and all the possible L_i , we can find and represent all the possible $(m-2)$ -dimensional faces (for instance, $L_i \cap L_j$ can be represented by an array containing the parameters defining both L_i and L_j). A similar procedure can be used for the other ℓ -dimensional faces.

Example 8.2. Given a vertex u with a given combinatorial representation, its neighbor vertices can be found by observing that if u and v are neighbors, then they are located on the same 1-dimensional face. This face is the intersection of $m-1$ hyperplanes. Hence for finding the neighbor vertices of u we simply need to go over the list of vertices v and choose the ones whose combinatorial representation contains $m-1$ hyperplanes which also appear in the representation of u .

9. SEVERAL THEORETICAL AND PRACTICAL ASPECTS

This section discusses several theoretical and practical aspects related to the algorithm. For the sake of convenience of the reading, the section is divided to a few subsections.

9.1. The model of computation: The model of computation is a one in which each of the processing units can work independently of the other ones and that the list of sites is available to all units (a shared memory for the list of sites). The analysis below can be (slightly) modified to the case where more memory cells are shared between several (perhaps all) processing units.

A further assumption in the model is that arithmetic operations (e.g., comparisons of two numbers), array manipulations, etc., are $O(1)$ independently of n . This assumption is implicit in the analyses of the time complexity of many geometric algorithms, including all of the Voronoi algorithms we aware of. In particular, this assumption implies that each number is represented by at most $MaxBit$ bits for some known and fixed number $MaxBit$ (say, 64 or 8196), an assumption which holds true in standard computers and widely used data structures (different data types, e.g., “int” and “double”, may be represented using a different number of bits, but $MaxBit$ is an upper bound on the sizes of all of these types). However, this assumption casts a (very large) strict upper bound on the size of the input n , namely $n \leq 2^{MaxBit}$. If one wants to take into account the case where arithmetic operations

depend on n (including the number of digits after the floating point) and if an unlimited number of memory cells is available, then a multiplying factor expressing this dependence (e.g., $O(\log(n))$) should be added to all of the complexity results in Theorem 9.1 below, as well as to all of the corresponding complexity results in the literature.

9.2. A time complexity theorem. The following theorem describes several aspects related to the algorithm.

Theorem 9.1. *Suppose that the world $X \subset \mathbb{R}^2$ is a compact and convex subset whose boundary is polygonal. Assume also that the distinct point sites p_1, \dots, p_n are contained in its interior. Then:*

- (a) *Algorithm 1 is correct. More specifically, given any site $p = p_k$, the computation of the Voronoi cell of p by Algorithm 1 terminates after a finite number of steps and the corresponding entries in the output of the algorithm include all the vertices and edges of the cell;*
- (b) *the time complexity, for computing one cell, is bounded above by $O(r_k e_k)$, where r_k is the maximum number of distance comparisons done along each shot ray (compared between all rays in a given cell), and e_k is the number of edges of the cell;*
- (c) *the time complexity, for the whole diagram, assuming one processing unit is involved, is bounded above (not necessarily tightly) by $O(n^2)$;*
- (d) *the time complexity, for the whole diagram, assuming Q processing units are involved (independently) and processor Q_i computes a set A_i of cells, is*

$$\max\left\{\sum_{k \in A_i} O(r_k e_k) : i \in \{1, \dots, Q\}\right\}.$$

- (e) *Let $\epsilon \in (0, 1)$ be given. Suppose that X is a rectangle and that there are $n > 16$ sites in X which are distributed independently of each other and according to the uniform distribution. Suppose further that n is large enough so that the following inequalities hold:*

$$\alpha_1 < \frac{1}{3} (\lfloor 0.2m \rfloor + 2), \tag{9.1}$$

$$\alpha_2 < e^{-2} (\lfloor 0.2m \rfloor + 1) \tag{9.2}$$

where

$$m := (\lfloor \sqrt{n} \rfloor)^2, \tag{9.3}$$

$$\alpha_1 := \left(\left\lfloor \sqrt{\ln \left(\frac{n(1 + 2e^{-400})}{\epsilon} \right)} \right\rfloor + \text{OneTwo} \right)^2, \tag{9.4}$$

$$\text{OneTwo} = \begin{cases} 1 & \text{if } \left\lfloor \sqrt{\ln \left(\frac{n(1 + 2e^{-400})}{\epsilon} \right)} \right\rfloor \text{ is even,} \\ 2 & \text{otherwise} \end{cases} \tag{9.5}$$

$$\beta := \frac{\sqrt{\alpha_1} - 1}{2}, \tag{9.6}$$

$$\alpha_2 := (1 + \lfloor 8\sqrt{2}(\beta + 1.01) \rfloor)^2. \quad (9.7)$$

Let m_1 and m_2 be any natural numbers satisfying

$$m_1 m_2 = m, \quad \min\{m_1, m_2\} > 2\sqrt{\alpha_2}, \quad (9.8)$$

e.g., $m_1 = m_2 = \sqrt{m}$ (from (9.2) it follows that $\sqrt{m} > 2\sqrt{\alpha_2}$). Suppose that a preprocessing stage is done in which X is decomposed into $m_1 \cdot m_2$ small squares. Then for all $k \in K$ and all rays shot during the computation of the cell of p_k using an improvement of Method 5.1 (namely, Method 10.2 below), one has that $r_k \leq 3\alpha_2$ with probability which is at least $1 - \epsilon$. The total number of distance comparisons done using Algorithm 1 for the computation of all of the Voronoi cells is at most $(3\alpha_2 - 1) \cdot 11n = O(n \log(n/\epsilon))$ with probability which is at least $1 - \epsilon$.

Remark 9.2. Here are a few comments regarding Theorem 9.1(e). First, the parameter OneTwo is needed only to ensure that α_1 is an odd number so that β will be an integer, and also that $\sqrt{\alpha_1} > \lfloor \sqrt{\ln(n(1 + 2e^{-400})/\epsilon)} \rfloor$ because of a technical reason needed in the proof. Second, the number 1.01 which appear in (9.7) is somewhat arbitrary: any number greater than 1 is OK, say 1.00000001. Third, the conditions (9.1)-(9.2) are always satisfied for large enough n because the floor function $\lfloor \cdot \rfloor$ grows at the same rate as the identity function and for given arbitrary $\tau_1, \tau_2, \tau_3 > 0$, one has $\lim_{n \rightarrow \infty} (\tau_1 n / \ln^{\tau_2}(\tau_3 n)) = \infty$. Fourth, it may worth substituting some values in the various parameters involved in the theorem. For instance, if $200000 \leq n \leq 10^{100}$ and $\epsilon = 0.000001$, then (9.1)-(9.2) are satisfied and with probability which is at least 0.999999 not greater than $343332n$ distance comparisons are made in the computation of all of the Voronoi cells.

Fifth, it may worth elaborating a bit on the notion of “with high probability” because in the computational geometry literature it is frequent to see the notion “on the average” (or “expected” or “in expectation”) which is a considerably different notion. Indeed, consider for instance n balls which are put in n boxes so that each ball has the same probability $1/n$ to be in each box and the balls are independent, i.e., we are in the case of uniform distribution. Elementary considerations show that the expected number of balls in each box is 1. However, the probability that in each box there is exactly one ball is $n!/n^n$. As follows from Stirling’s formula (11.4), this number tends exponentially fast to 0 as n tends to infinity. In other words, although on the average there is one ball in each box, the probability that a random configuration (according to the uniform distribution) of balls in the boxes leads to exactly one ball in each box is very low. Hence, although there are “linear expected time” algorithms for computing the Voronoi diagram of uniformly distributed sites [13, 38], it definitely does not mean, and actually has never been proved mathematically, that with high probability they do at most a linear number of calculations when computing the Voronoi diagram of a random configuration of sites.

9.3. Ideas behind the proof: The proof of Theorem 9.1 is quite technical (see Section 11), but the main idea regarding the bound on the time complexity is simple: each time a ray is shot, a new edge of the cell is detected, or a vertex is found, or the

subcone induced by the ray and another ray does not contain vertices. This shows (after a careful counting) that the number of rays used for each cell is bounded by a universal constant times the number of edges in the cell. The operations done along a given ray for detecting its endpoint are mainly distance comparisons (or some $O(1)$ operations). The maximum number of such operations, compared between all the shot rays, is r_k , and the upper bound follows. As for the upper bound on the whole diagram, one observes that the total number of edges is of the order of the size of the diagram and recalls the well known fact that this size is $O(n)$ (see also the proof of Lemma 11.6). Since r_k is bounded by $O(n)$ (for each k), the bound $O(n^2)$ follows. When the sites are distributed independently of each other and according to the uniform distribution, then with high probability all the endpoints will be not far from their site p_k (when they are far then they are closer to other sites and hence outside the cell of p_k). More careful estimates show that $r_k = O(\ln(n/\epsilon))$ and the bound $O(n \ln(n/\epsilon))$ follows. We believe that a linear upper bound can be given: see Section 12.

9.4. Possible improvements: It is not clear whether the bound on the time complexity presented in Theorem 9.1 is tight, after possibly taking into account several enhancements, but we believe that such enhancements may give better bounds or better constants (at least in the one processor case): for example, perhaps by computing the cells in a certain order (e.g., using plan sweep), by improving the endpoint computation (Method 5.1), etc. See Section 10 for a discussion on an improvement using bucketing technique which implies the $O(n)$ time complexity in the case of uniform distribution of sites.

9.5. Serial time complexity: a comparison to other algorithms: The upper bound on the worst case serial time complexity (one processing unit is involved) is at least as good as the bound $O(n^2)$ of the incremental method [46], [59], [60, pp. 242-251]. The bound is also better than the corresponding bound of the naive method [60, pp. 230-233] which is $O(n^2 \log(n))$. On the other hand, it is worse than the $O(n \log(n))$ of some algorithms (plan-sweep, divide and conquer, the method based on convex hulls) [9]. It should be emphasized however that it is still not known that the established upper bound is tight (Subsection 11.3), and in addition, even if it is tight, then the main advantage of our algorithm is in its natural ability to support simple parallel computing in various ways (see Subsection 9.7). Furthermore, in common scenarios (uniform distribution of sites) there is a high probability of linear behavior (Subsection 11.3, Section 9.6).

9.6. Serial time complexity: worst case against common scenarios: The difference between the potential worst case scenarios and the common one is similar in some sense to the Quicksort algorithm for sorting [30, 51] whose average time complexity is $O(n \log(n))$ but its worst case time complexity is $O(n^2)$. The simplex algorithm for linear programming [32, 33] provides another example (efficient in practice, with polynomial average case complexity [76], but exponential time complexity in the worst case [54]). Related phenomena occur in the Voronoi case, e.g.,

the average case complexity $O(n \log(n))$ of the incremental method [48] against the $O(n^2)$ worst case.

9.7. Parallel time complexity: So far it was assumed that only one processing unit is involved. If Q processing units are involved in the computation of the whole diagram, and processor Q_i computes a set A_i of cells, then the time complexity is $\max\{\sum_{k \in A_i} O(r_k e_k) : i \in \{1, \dots, Q\}\}$. Similarly to the explanation given in Subsection 11.3, it can be shown that when the sites are (independently) uniformly distributed, then with probability $1 - \epsilon$ one has $O(r_k e_k) = O(\log(n/\epsilon)e_k)$ (in practice $r_k \leq 50$ and $e_k \leq 20$; for most cells actually $e_k = 6$) and the time complexity becomes $\max\{\sum_{k \in A_i} O(\log(n/\epsilon)e_k) : i \in \{1, \dots, Q\}\}$. In the above analysis it was assumed that each cell is computed by one processor. The advantage of our algorithm is that it also allows parallelizing of the computation of each cell, since each subcone can be handled independently of other subcones and so the work can be divided by several processors.

Returning back to the worst case scenario, one may want to avoid cases where a certain large cell slows the whole computation. To avoid this, if a certain processing unit detects a cell having too many sides (e.g., more than 20), then it can halt its work and go to other cells. The sides and vertices of the problematic cell will be found using neighbor cells and will be constructed almost automatically at the end. Alternatively, additional processing units can help to compute the problematic cell.

10. IMPROVEMENT OF THE ALGORITHM FOR THE CASE OF UNIFORM DISTRIBUTION OF SITES

This section describes an improvement of Method 5.1. This method is general in the sense that it can be used for any type of distribution of the sites. However, it is most efficient for the case where the sites are distributed independently according to the uniform distribution, i.e., the probability of each site to be in some region is proportional to the area of the region, and there is no dependence between the sites (when viewed as random vectors). We assume that X is a rectangle whose side lengths are integer multiplications of some real number $s > 0$. A rough description of the method is as follows. We first perform a preprocessing stage whose complexity is $O(n)$ in which the sites are inserted into a corresponding data structure (buckets) mentioned in [13]. When computing the Voronoi cell of some site p , the buckets allow us to restrict the distance comparisons to sites located near the temporary endpoint y (up to distance $d(p, y)$), since according to Lemma 10.5 below farther sites a will automatically satisfy $d(y, a) > d(y, p)$ and hence there is no need to consider them. The buckets also help us to find a candidate to the first temporary endpoint which is usually close to p , since unless some square around y is empty of sites (very low probability: see Subsection 11.3), Lemma 10.6 below ensures that farther sites a will automatically satisfy $d(y, a) > d(y, p)$. The rest of the method is as Method 5.1.

We will use the following terminology. We denote by $B[y, r]$ the disk of radius $r > 0$ and center $y \in \mathbb{R}^2$ and by $S[y, r]$ the square of radius $r > 0$ and center $y \in \mathbb{R}^2$,

i.e., $S[y, r] = \{x \in \mathbb{R}^2 : |x - y|_\infty \leq r\}$ where $|(w_1, w_2)|_\infty = \max\{|w_1|, |w_2|\}$ is the ℓ_∞ norm of a point $w \in \mathbb{R}^2$. The integer square $S_I[y, r]$ is the rectangle defined as follows:

$$S_I[y, r] := [s\lfloor(y_1 - r)/s\rfloor, s(\lfloor(y_1 + r)/s\rfloor + 1)] \times s[\lfloor(y_2 - r)/s\rfloor, s(\lfloor(y_2 + r)/s\rfloor + 1)]. \quad (10.1)$$

Here $\lfloor \cdot \rfloor$ is the floor function, i.e., $\lfloor t \rfloor$ is the largest not exceeding $t \in \mathbb{R}^2$. See Figures 9-10 for an illustration. Usually $S_I[y, r]$ is the smallest rectangle which contains $S[y, r]$ and composed of small squares. The exceptions are when $S[y, r]$ is composed of small squares and then $S_I[y, r]$ contains one more column to the right (unless the rightmost boundary of $S[y, r]$ coincides with the boundary of X) and one more row to the up (unless the uppermost boundary of $S[y, r]$ coincides with the boundary of X). It is convenient to work with the integer square for theoretical analysis and this is what will be done from now on. However, we remark briefly that for the programming work it is more convenient to work with the discrete integer square $\hat{S}_I[y, r] := [\lfloor(y_1 - r)/s\rfloor, \lfloor(y_1 + r)/s\rfloor]_I \times [\lfloor(y_2 - r)/s\rfloor, \lfloor(y_2 + r)/s\rfloor]_I$, where the segment $[t_1, t_2]_I$ means all the integers between the real number t_1 and the real number t_2 . The discrete square represents the pairs of indices contained in the integer square $S_I[y, r]$.

Method 10.1. (Preprocessing)

- (1) Decompose X into $m_1 \cdot m_2$ small squares (buckets), where $m_1, m_2 \in \mathbb{N}$ and each small square is of side length s .
- (2) Associate each site $a = (a_1, a_2)$ to the small square containing it and having the lowest indices, i.e., the indices are $i_j = \lfloor a_j/s \rfloor$, $j \in \{1, 2\}$.
- (3) Enlarge the grid of small squares around X by some width (depending on the user), where each small square in this grid is defined to be empty of sites.

The last step in Method 10.1 is performed in order to avoid complications when some rectangles go out of X . This last stage can be avoided by working with the intersection of integer squares and X but this complicates the programming and the analysis.

We now describe Method 10.2 which improves upon Method 5.1. Its theoretical justification is described in the remarks and lemmas mentioned after it. The justification of the probabilistic part is given in Subsection 11.3.

Method 10.2. (Improved endpoint computation)

- **Input:** The sites in a bucketing data structure; a site p ; a unit vector θ ; an integer $\beta > 0$.
 - **Output:** the endpoint $p + T(\theta, p)\theta$.
- (1) Let $\eta := 2\sqrt{2}(\beta + 1.01)s$ and $y := p + \eta\theta$ and let $y_X := p + t\theta$ be the intersection of the ray of θ with the boundary of X (see Remark 5.2 regarding the computation of y_X).
 - (2) If $\eta > t$, then y is outside X and we let $y := y_X$. From now on $\eta \leq t$.
 - (3) If the distance $d(y, \partial X)$ between y and the boundary of X satisfies $d(y, \partial X) \geq \beta s$, then $S_I[y, \beta s] \subseteq X$ and we check whether $d(p, y) \leq d(y, a)$ for all sites

- $a \in S_I[y, \beta s]$. If yes (very low probability), then we let $y := y_X$. Otherwise, y is outside the cell of p .
- (4) If $d(y, \partial X) < \beta s$, then let $y := p + 2\eta\theta$. Either y is in X or not.
 - (5) If not, equivalently, if $2\eta > t$, then we let $y := y_X$.
 - (6) If $y \in X$, then we construct $S_I[y, 2\beta s]$ and check whether $d(y, p) \leq d(a, y)$ for all sites $a \in S_I[y, 2\beta s]$. If yes (very low probability because at least quarter of $S[y, 2\beta s]$ is inside X , and this quarter is a square of side length $(2\beta + 1)s$), then we let $y := y_X$. Otherwise, y is outside the cell of p .
 - (7) The point y obtained at the end of the previous steps is the first temporary endpoint.
 - (8) If y is known to be outside the cell, then go to Step (11). Otherwise, let L be the boundary line on which y is located (either a bisector or a facet of X).
 - (9) Check whether y is in the cell by comparing $d(y, p)$ to $d(y, a)$ for all sites $a \in S_I[y, d(p, y)]$, possibly with enhancements which allow to reduce the number of distance comparisons.
 - (10) If y is in the cell, then y is the endpoint and L is the bisecting line. The calculation along the ray is complete;
 - (11) otherwise, $d(y, a) < d(y, p)$ for some site a . Let $CloseNeighbor := a$.
 - (12) Find the point of intersection (call it u) between the given ray and the bisecting line L between p and $CloseNeighbor$. This intersection is always nonempty. The line L can be easily found because it is vertical to the vector $p - CloseNeighbor$ and passes via the point $(p + CloseNeighbor)/2$.
 - (13) let $y := u$; go to Step (9).

For some illustrations, see Figures 9-10.

Remark 10.3. Here are a few comments regarding some of the steps in Method 10.2. First, as already mentioned in Remark 9.2, the number 1.01 in Step (1) and also in (9.7) is somewhat arbitrary. It can be replaced by any number greater than 1, e.g., 1.0000001. See the proof of Lemma 10.6. The distance comparisons in Method 10.2 Step (2) can be done, e.g., by starting with the small square of y (shell 0), then checking the 8 squares around this small square (shell 1), then going to shell 2, i.e., the shell of 16 squares around shell 1, and so forth.

Lemma 10.4. *Let $p, y \in X$, $p \neq y$. Let $B[y, d(p, y)]$ be the disk of radius $d(p, y)$ and center y . If y' is in the segment $[p, y]$, then the disk $B[y', d(p, y')]$ is contained in $B[y, d(p, y)]$ and the integer rectangle $S_I[y', d(p, y')]$ is contained in the integer rectangle $S_I[y, d(p, y)]$.*

Proof. Let $x \in B[y', d(p, y')]$. From the triangle inequality

$$d(x, y) \leq d(x, y') + d(y', y) \leq d(p, y') + d(y', y) = d(p, y)$$

because $y' \in [p, y]$. Thus $x \in B[y, d(p, y)]$. Since x was arbitrary, the inclusion $B[y', d(p, y')] \subseteq B[y, d(p, y)]$ holds.

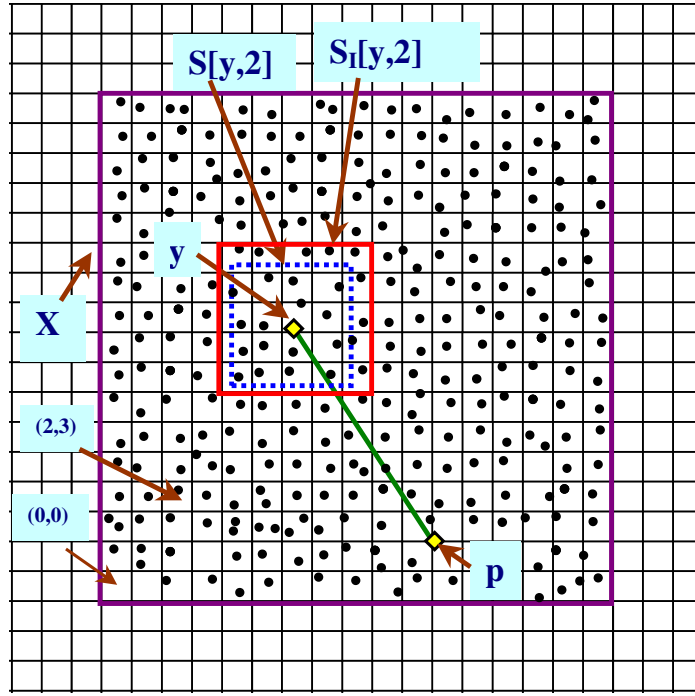


FIGURE 9. An illustration of issues related to Method 10.2.

To see the inclusion $S_I[y', d(p, y')] \subseteq S_I[y, d(p, y)]$ we observe from (10.1) that $S_I[y, d(p, y)] = J_1 \times J_2$ and $S_I[y', d(p, y')] = J'_1 \times J'_2$ where

$$J_j := [s \lfloor (y_j - d(p, y))/s \rfloor, s(\lfloor (y_j + d(p, y))/s \rfloor + 1)], \quad (10.2)$$

$$J'_j := [s \lfloor (y'_j - d(p, y'))/s \rfloor, s(\lfloor (y'_j + d(p, y'))/s \rfloor + 1)], \quad (10.3)$$

and $j \in \{1, 2\}$, $y' = (y'_1, y'_2)$. The point $y' - d(p, y')(1, 0)$ is in $B[y', d(p, y')]$, thus it is in $B[y, d(p, y)]$ from the previous paragraph. Hence $d(y' - d(p, y')(1, 0), y) \leq d(p, y)$ and thus $|y_1 - (y'_1 - d(p, y'))| \leq d(p, y)$. Therefore $y_1 - d(p, y) \leq y'_1 - d(p, y')$. Similarly the points $y' + d(p, y')(1, 0)$, $y' - d(p, y')(0, 1)$, $y' + d(p, y')(0, 1)$ are in $B[y, d(p, y)]$ and the following inequalities hold

$$y'_1 + d(p, y') \leq y_1 + d(p, y), \quad y_2 - d(p, y) \leq y'_2 - d(p, y'), \quad y'_2 + d(p, y') \leq y_2 + d(p, y).$$

Since the floor function $\lfloor \cdot \rfloor$ is increasing on \mathbb{R} , the previous inequalities and (10.2)-(10.3) imply the inclusion $S_I[y', d(p, y')] \subseteq S_I[y, d(p, y)]$. \square

Lemma 10.5. *Consider a site p and a ray emanating from p in the direction of θ . Let $y \in X$ be a temporary endpoint obtained in Method 10.2. When applying Method 10.2 and performing distance comparisons for computing the next temporary endpoint (or for verifying that y is a permanent endpoint), it is sufficient to consider sites in the integer square $S_I[y, d(p, y)]$. Moreover, for all possible such temporary endpoints y all of the corresponding considered sites are in $S_I[y_0, d(p, y_0)]$, where $y_0 \in X$ is the first temporary endpoint obtained in Method 10.2.*

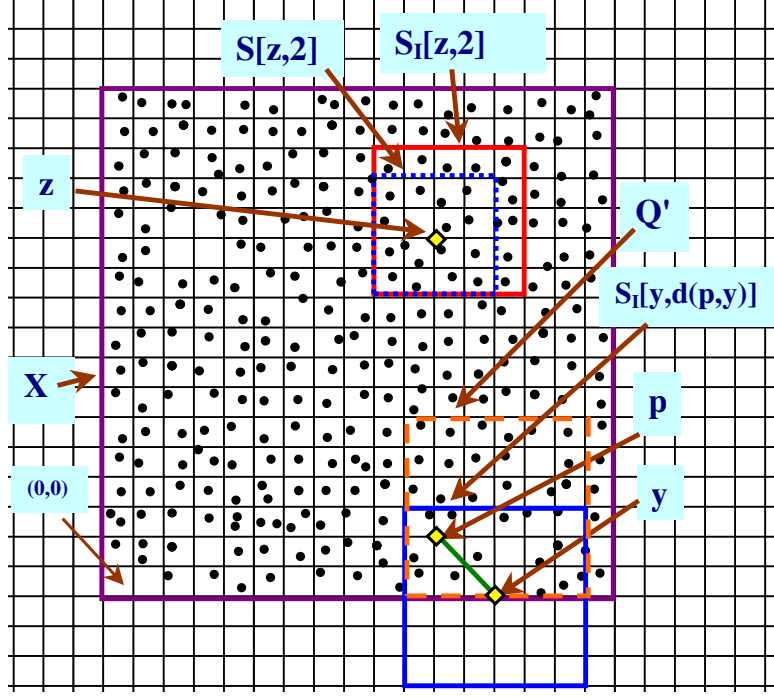


FIGURE 10. Another illustration of issues related to Method 10.2. Here Q' is an integer square contained in X and contains $X \cap S_I[y, d(p, y)]$. It also contains the same number of small squares as $S_I[y, d(p, y)]$.

Proof. Let y be a temporary endpoint obtained from Method 10.2. Let $a \in X$ be a site satisfying $a \notin S_I[y, d(p, y)]$. We claim that automatically $d(a, y) > d(p, y)$, and hence the distance comparison between $d(a, y)$ and $d(p, y)$ is redundant. Indeed, let $x \in B[y, d(p, y)]$. Then $|x - y| \leq d(p, y)$. Since for the Euclidean norm $|\cdot|$ and the ℓ_∞ norm $|\cdot|_\infty$ we have $|w|_\infty \leq |w|$ for all $w \in \mathbb{R}^2$, it follows that $|x - y|_\infty \leq d(p, y)$. Therefore $B[y, d(p, y)] \subseteq S[y, d(p, y)]$. By definition $S[y, d(p, y)] \subseteq S_I[y, d(p, y)]$. We conclude that $B[y, d(p, y)] \subseteq S_I[y, d(p, y)]$, and hence, from the choice of a , we have $a \notin B[y, d(p, y)]$. The first assertion follows.

As for the second assertion, let y be an arbitrary endpoint. The behavior of Method 10.2 implies that $y \in [p, y_0]$. We already know that we need to consider only sites in $S_I[y, d(p, y)]$. Let a be an arbitrary site in $S_I[y, d(p, y)]$. It follows from Lemma 10.4 that $a \in S_I[y_0, d(p, y_0)]$ and the assertion follows since y and a were arbitrary. \square

Lemma 10.6. *Let $p \in \mathbb{R}^2$ and a unit vector θ be given. Let $\beta \in \mathbb{N}$, $s > 0$, $y := p + 2\sqrt{2}(\beta + 1.01)s\theta$. Then any $x \in S_I[y, \beta s]$ satisfies $d(x, y) < d(x, p)$.*

Proof. Since $x \in S_I[y, \beta s]$, the definition of $S_I[y, \beta s]$ implies that $|x - y|_\infty \leq (\beta + 1)s$. Since $|z| \leq \sqrt{2}|z|_\infty$ for all $z \in \mathbb{R}^2$, we have $|x - y| \leq \sqrt{2}(\beta + 1)s$. Thus $x \in$

$B[y, \sqrt{2}(\beta + 1)s]$. Since

$$|y - p| - \sqrt{2}(\beta + 1)s > 2\sqrt{2}(\beta + 1)s - \sqrt{2}(\beta + 1)s = \sqrt{2}(\beta + 1)s \geq |x - y|,$$

it follows in particular that $|y - p| - \sqrt{2}(\beta + 1)s > 0$ and hence $p \notin B[y, \sqrt{2}(\beta + 1)s]$ and the distance between p and $B[y, \sqrt{2}(\beta + 1)s]$ is $|y - p| - \sqrt{2}(\beta + 1)s$. Because $x \in B[y, \sqrt{2}(\beta + 1)s]$ the distance between p and x is at least $d(p, B[y, \sqrt{2}(\beta + 1)s])$. All the above implies that $d(x, p) \geq d(p, B[y, \sqrt{2}(\beta + 1)s]) > d(x, y)$ as claimed. \square

11. PROOF OF THEOREM 9.1

In this section we prove Theorem 9.1 which shows the correction of the algorithm and presents an upper bound on its time complexity. The proof is long and is based on several lemmas. The first lemmas (Lemmas 11.1-11.11) are related to the proof of the upper bound on the time complexity, and the other lemmas (Lemmas 11.12-11.15) are related to the correctness of the output of the algorithm. The proof of Theorem 9.1(e) is given in Subsection 11.3.

Here are additional details regarding notation and terminology. In the sequel $p = p_k$ is a given site. As already mentioned, we assume that all the sites are distinct, known in advance, and no site is located on the boundary of the world X . In particular $\min\{d(p_k, p_j) : k \neq j\} > 0$. Since the distance between p and the boundary of the cell is positive, there is a small circle with center p which is contained in the interior of the cell. On this circle we construct the simplex, which, as a consequence, has a positive distance from the boundary of the cell and from p . Any other simplex which may be used in the algorithm for producing the rays and detecting the vertices is simply a scalar multiplication of this small simplex and it produces exactly the same rays (hence enables to detect the same vertices). Recall again that we use the notion “facet” for denoting an edge of the cell (a side).

A vertex v of the cell is said to correspond to a subfacet F of the simplex if v is located inside the cone corresponding to F . For instance, in Figure 5 the vertex v corresponds to the subfacet $F = \{\theta_1, \theta_3\}$ and no other vertices correspond to F . All the rays we consider emanate from a given site $p = p_k$ and are sometimes identified with their direction vectors. Given a cone generated by two rays, the rays on the boundary of the cone are called boundary rays and any other ray in the cone is called an intermediate ray. For instance, in Figure 5 if we look at the cone generated by θ_1 and θ_2 , then these rays are boundary rays and θ_3 is an intermediate ray. Continuing with Figure 5, after additional steps additional rays will be generated between θ_1 and θ_3 , and hence they will be intermediate rays in the cone generated by θ_1 and θ_2 (and also of the one generated by θ_1 and θ_3). Between θ_1 and θ_3 no additional rays will be generated.

Part of the proof is to analyze the time complexity of the algorithm and in particular to prove that the algorithm terminates after finitely many steps. For doing this it is convenient to consider the algorithm tree, namely the graph whose nodes are the main stages in the algorithm, and a node has subnodes (children nodes) whenever a conditional operation (separating into cases, if-else, etc.) is made in the node whose result is a non-terminating-condition statement (i.e., further work is required

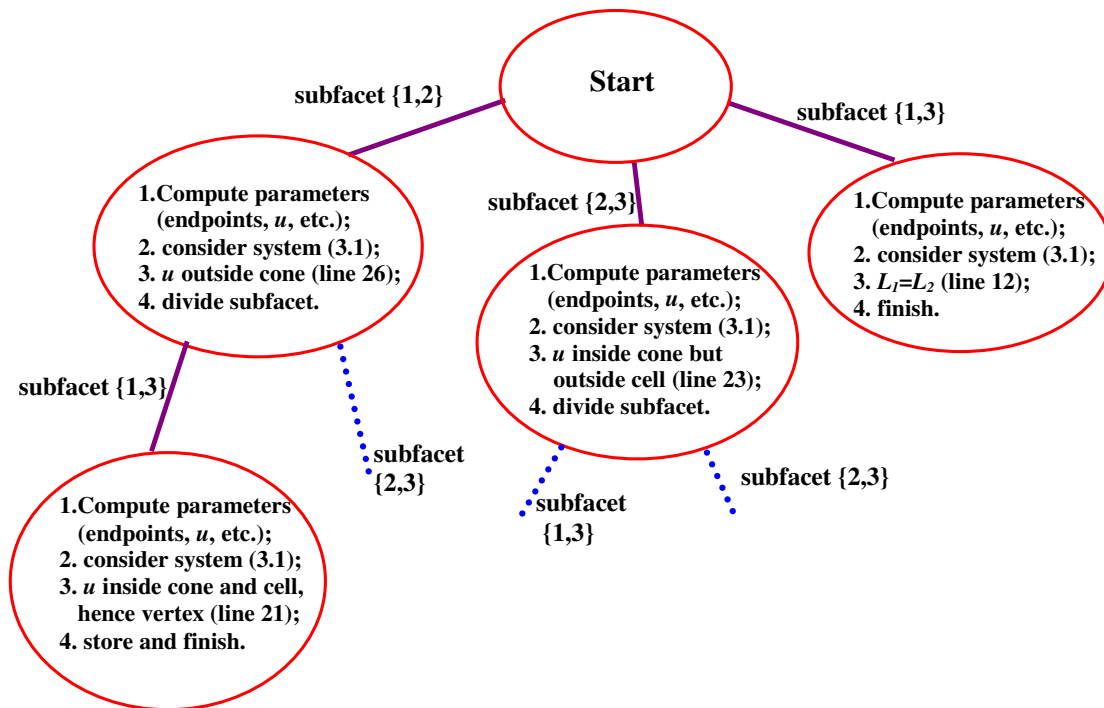


FIGURE 11. Illustration of the algorithm tree for the cell of Figure 4.

by the algorithm to achieve a terminating condition). Once we are given an upper bound on the number of nodes in the tree and on the number of operations done in each node, we have an upper bound on the time complexity of the algorithm. See Figure 11 for an illustration of the algorithm tree for the cell described in Figure 4.

In Algorithm 1 there are two types of nodes: in the first type (lines 12 and 21) the algorithm finishes its consideration with the current subfacet (perhaps after storing some information) without further dividing it. In the second type (lines 14, 23, and 26) the subfacet is divided into two subfacets and the algorithm continues with both of them. In other words, in the first type there are no children nodes and in the second one there are. For the sake of simpler analysis, the computation of the two endpoints done in line 6 (or passing them in a computed form from previous stages), a computation which is done before each conditional operation, is considered as performed in each node and not in a separated node. If, for the sake of fully counting the number of nodes, such a computation is considered in a separate node, then the total number of nodes will be greater by at most a factor of 2 than in our analysis since before each of the two types of nodes mentioned above there is only one “endpoint computation node”.

11.1. Serial and parallel time complexity (without improvement).

Lemma 11.1. *Consider a simplex subfacet $F = \{\theta_1, \theta_2\}$ and the corresponding cone generated from it. Let L_1 and L_2 be the lines on which the endpoints $p + T(\theta_i, p)\theta_i$, $i = 1, 2$ are located. Suppose that an intermediate ray in the direction of θ_3 is generated when F is considered. Then the ray of θ_3 hits a facet different from $\widetilde{L}_i, i = 1, 2$.*

Proof. First note any ray generated by the algorithm does hit a facet \widetilde{L}_3 . Indeed, the ray starts at a point inside the cell and goes outside the cell, possibly outside the region X (because X is bounded). Thus the intermediate value theorem implies that this ray intersects the boundary of the cell, namely, a certain facet \widetilde{L}_3 (the point hit by the ray is $p + t\theta$ where θ is a unit vector in the direction of the ray and $t = \sup\{s \in [0, \infty) : p + s\theta \text{ in the cell}\}$).

Denote by g the point hit by the ray. This point is in fact the endpoint. Indeed, by the definition of the endpoint (see (2.1)) the ray of θ_3 has an endpoint $p + T(\theta_3, p)\theta_3$. Any point on the ray after g is strictly outside the cell (either because it is outside the world or because it is in a halfspace of another site). Thus $p + T(\theta_3, p)\theta_3 \in [p, g]$. However, any point beyond $[p, p + T(\theta_3, p)\theta_3]$ is outside the cell by the definition of the endpoint. Since we know that g is in the cell (it belongs to the facet \widetilde{L}_3) we obtain that $g \in [p, p + T(\theta_3, p)\theta_3]$. Thus $g = p + T(\theta_3, p)\theta_3$.

Now we observe that an intermediate ray is created only when either L_1 and L_2 are parallel (line 14), or when they intersect in the cone but outside the cell (line 23), or when they intersect outside the cone (line 26).

In the first case the line on which the ray of θ_3 is located is parallel to L_1 and L_2 , and hence cannot hit them. In particular $\widetilde{L}_3 \neq \widetilde{L}_i, i = 1, 2$.

Now consider the second case and suppose for a contradiction that, say, $\widetilde{L}_1 = \widetilde{L}_3$. Let $u = L_1 \cap L_2$. By assumption u is outside the cell. In particular u is hit by the ray of θ_3 (see line 23) and $u \neq p + T(\theta_3, p)\theta_3$. But both u and $p + T(\theta_3, p)\theta_3$ are assumed to belong to \widetilde{L}_1 and hence to L_1 . Since a line is fully determined by two distinct points on it, L_1 contains the ray of θ_3 and in particular passes via p . This is impossible since p is in the interior of the cell and hence its distance to any of the boundary lines is positive.

Now consider the third case and suppose for a contradiction that, say, $\widetilde{L}_1 = \widetilde{L}_3$. Let $u = L_1 \cap L_2$. By assumption u is outside the cone generated by the rays of θ_1 and θ_2 . Since θ_3 is in the direction of $p - u$ (see line 27), it does not hit u and hence $u \neq p + T(\theta_3, p)\theta_3$. But both u and $p + T(\theta_3, p)\theta_3$ are assumed to belong to \widetilde{L}_1 and hence to L_1 . Since a line is fully determined by two distinct points on it, L_1 contains the segment $[u, p + T(\theta_3, p)\theta_3]$ and in particular it passes via p . This is impossible since p is in the interior of the cell and hence its distance to any of the boundary lines is positive. \square

Lemma 11.2. *Consider two different rays generated by the algorithm, say in the direction of ϕ_1 and ϕ_2 . These rays may belong to different simplex subfacets but both of them are assumed to be between (and possibly coincide with) two initial rays, i.e., rays induced by two corners of the simplex. Consider an intermediate ray between*

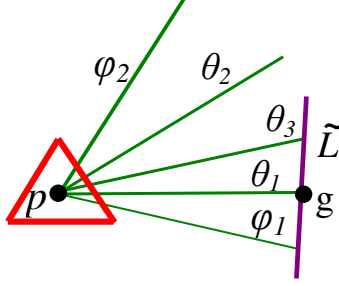


FIGURE 12. An illustration of Lemma 11.2.

the rays of ϕ_i , $i = 1, 2$ whose direction vector is θ_3 . Then the endpoint of the ray of θ_3 and the endpoints of the rays of ϕ_1 and ϕ_2 must be located on different facets.

Proof. Suppose to the contrary that this is not true, say the endpoint of the ray of ϕ_1 and the endpoint of the ray of θ_3 are located on the same facet \tilde{L} . Because the ray of θ_3 is between two initial rays it is generated from some subfacet $\{\theta_1, \theta_2\}$. Here θ_1 is between ϕ_1 and θ_3 and possibly equals ϕ_1 , and θ_2 is between θ_3 and ϕ_2 and possibly equals ϕ_2 . This generation corresponds to the routines of lines 14, 26, or 23 of the algorithm and in particular $\theta_1 \neq \theta_3$ and $\theta_2 \neq \theta_3$. Denote by \tilde{L}_i , $i = 1, 2$ the facets on which the endpoints corresponding to θ_i , $i = 1, 2$ are located.

The ray of θ_1 intersects \tilde{L} at some point g which is its endpoint as explained in the proof of Lemma 11.1. See also Figure 12. We conclude that the endpoints of the rays of θ_3 and of θ_1 are located on the same facet. But this is impossible, since by assumption θ_3 was created from the simplex subfacet $\{\theta_1, \theta_2\}$ and as already mentioned, this can happen only when either L_1 and L_2 are parallel (line 14), or when they intersect outside the cone (line 26) or when they intersect in the cone but outside the cell (line 23), and in all of these cases the ray of θ_3 hits a facet different from the ones associated with θ_1 and θ_2 (see Lemma 11.1). We arrived at a contradiction which proves the assertion. \square

Lemma 11.3. *The algorithm terminates after a finite number of steps. In particular, the number of intermediate rays is finite.*

Proof. This follows from Lemma 11.2. Indeed, suppose for a contradiction that the algorithm does not terminate after finitely many steps. This means that the list of simplex subfacets *FacetQueue* is never empty. But in each stage of the algorithm (each node), either a subfacet is divided (lines 14, 23, and 26) and then replaced by its children subfacets and deleted from *FacetQueue*, or it has no children subfacets (lines 12 and 21) and hence it is deleted from *FacetQueue* shortly after its creation. After a subfacet is deleted from *FacetQueue* it is never created again. As a result, the fact that the algorithm does not terminate after finitely many steps implies that we can find an infinite sequence of nested distinct subfacets. When a subfacet is created a new edge of the cell is detected (because of Lemma 11.2) and such an

edge could not be detected before, again because of Lemma 11.2. Thus infinitely many distinct edges are detected, contradicting the fact that each cell has only finitely many edges. Hence the algorithm terminates after finitely many steps and in particular finitely many intermediate rays are created. \square

Lemma 11.4. *Given a cone generated by two distinct unit vectors θ_1 and θ_2 (located between initial rays, possibly equal to the initial rays), let E be the number of facets of the cell hit by intermediate rays, i.e., rays produced by the algorithm inside the cone excluding the boundary rays of the cone. Then the tree of the restriction of the algorithm to the given cone contains exactly $2E + 1$ nodes.*

Proof. The proof is by induction on E . By Lemma 11.3 we know that E is finite. Let \widetilde{L}_i be the facet on which the endpoint $p + T(\theta_i, p)\theta_i$ is located, $i = 1, 2$. If $E = 0$, then there are two cases. In the first case the rays generated by θ_i , $i = 1, 2$ hit the same facet and in this case (line 12) the current simplex subfacet is deleted from *FacetQueue*. Thus no subnode of the current node is created, i.e., the restriction of the algorithm tree to the cone contains $1 = 2E + 1$ nodes. In the second case the rays must hit different facets which intersect at a vertex, since otherwise either no intersection occurs or the intersection is a point outside the cell or outside the cone, and the corresponding ray in the direction of θ_3 (lines 14, 23, 26) hits a facet contained in the cone, contradicting $E = 0$. Therefore also in this case the current subfacet is deleted from *FacetQueue* and no subnode of the current node is created and the restriction of the algorithm tree to the cone contains $2E + 1 = 1$ nodes.

Now assume that the claim holds for any nonnegative integer not exceeding $E - 1$, $E \geq 1$. It will be proved that it holds for E too. Indeed, if the current simplex subfacet $\{\theta_1, \theta_2\}$ is not divided into two subfacets $\{\theta_1, \theta_3\}$ and $\{\theta_2, \theta_3\}$, then the restriction of the algorithm tree to the cone generated by $\{\theta_1, \theta_2\}$ contains only one node and hence there cannot be any facet different from \widetilde{L}_1 and \widetilde{L}_2 which is hit by rays produced by the algorithm, contradicting the assumption that $E \geq 1$. Knowing that $\{\theta_1, \theta_2\}$ is divided, i.e., the root node has 2 children, consider the number of facets $e_{1,3}$ and $e_{2,3}$ of the cell contained in the cones generated by $\{\theta_1, \theta_3\}$ and $\{\theta_2, \theta_3\}$ respectively, excluding, in each cone, the facets (1 or 2) hit by the boundary rays. Since $E = e_{1,3} + e_{2,3} + 1$ (where the 1 comes from the facet hit by the ray in the direction of θ_3) it follows that $e_{1,3} < E$ and $e_{2,3} < E$. Thus the induction hypothesis implies that the trees of the restriction of the algorithm to the cones generated by the subfacets $\{\theta_1, \theta_3\}$ and $\{\theta_2, \theta_3\}$ contain exactly $2e_{1,3} + 1$ and $2e_{2,3} + 1$ nodes, respectively. Hence the tree generated by the restriction of the algorithm to the original cone (the one corresponding to $\{\theta_1, \theta_2\}$) contains $(1 + 2e_{1,3}) + (1 + 2e_{2,3}) + 1 = 2E + 1$ nodes, as claimed. \square

Lemma 11.5. *Given a cell of some site $p = p_k$, the restriction of the algorithm tree to this cell contains at most $2e_k - 1$ nodes, where e_k is the number of facets of the cell.*

Proof. Consider the 3 cones generated by the very initial rays, i.e., the rays shot in the direction of the corners of the simplex. The number of nodes in the algorithm

tree restricted to the cell is the sum of nodes in each of the trees corresponding to the above cones. By Lemma 11.4 we conclude that this number is $2(E_{1,2} + E_{2,3} + E_{1,3}) + 3$, where $E_{i,j}$, $i \neq j$, $i, j \in \{1, 2, 3\}$ are the number of facets hit by intermediate rays.

Note that a facet \tilde{L} cannot be hit by two intermediate rays belonging to two different initial cones. Indeed, assume to the contrary that this happens, say $\theta_{1,2}$ is the direction of an intermediate ray belonging to an initial cone generated by θ_1 and θ_2 , and $\theta_{2,3}$ is the direction of an intermediate ray belonging to an initial cone generated θ_2 and θ_3 . These two intermediate rays cannot be opposite, otherwise \tilde{L} will be parallel to itself (without coinciding with itself). Hence θ_2 is (strictly) in the linear cone generated by $\theta_{1,2}$ and $\theta_{2,3}$, that is $\theta_2 = \lambda_{1,2}\theta_{1,2} + \lambda_{2,3}\theta_{2,3}$ for some $\lambda_{1,2} > 0$ and $\lambda_{2,3} > 0$. The part of the facet \tilde{L} between the endpoints of the cone is the convex combination of them, i.e., the segment $[p + T(\theta_{1,2}, p)\theta_{1,2}, p + T(\theta_{2,3}, p)\theta_{2,3}]$.

A direct calculation shows that the ray of θ_2 intersects \tilde{L} at a unique point g : this is done by proving that there exist unique t and $\alpha \in (0, 1)$ satisfying

$$p + t\lambda_{1,2}\theta_{1,2} + t\lambda_{2,3}\theta_{2,3} = \alpha(p + T(\theta_{1,2}, p)\theta_{1,2}) + (1 - \alpha)(p + T(\theta_{2,3}, p)\theta_{2,3}) \quad (11.1)$$

by equating the corresponding coefficients. The point g belongs to the cell and hence it is located on the ray of θ_2 prior to the endpoint $p + T(\theta_2, p)\theta_2$. But any point on the ray after g is outside the cell since it is located either outside X (if \tilde{L} is a boundary edge of X) or in a halfspace of a different site. Thus $g = p + T(\theta_2, p)\theta_2$. This contradicts Lemma 11.2 which implies that the endpoint corresponding to θ_2 is located on a facet different from the ones corresponding to $\theta_{1,2}$ and $\theta_{2,3}$, i.e., different from \tilde{L} . We arrived at a contradiction which proves the assertion.

From the previous two paragraphs we can conclude that $E_{1,2} + E_{2,3} + E_{1,3} \leq e_k$. However, in fact we can conclude that

$$E_{1,2} + E_{2,3} + E_{1,3} \leq e_k - 2 \quad (11.2)$$

because the set of facets of the cell is the disjoint union of the set of facets hit by intermediate rays and the facets hit by the three initial rays, and this latter set contains at least two different facets. The assertion follows. \square

Lemma 11.6. *Consider the tree generated by the algorithm for the whole diagram. Let $|X|$ be the number of edges of the polygon X . Then the number of nodes in this tree is bounded above by $1 + (11 + 2|X|)n = O(n)$.*

Proof. The algorithm tree for the whole diagram is the union of the trees corresponding to each cell and an additional root node. By Lemma 11.5 the tree of the cell of p_k has at most $2e_k - 1$ nodes, where e_k is the number of facets of the cell. The set of facets of each cell can be written as the disjoint union of two sets: the set of facets located on the boundary of the polygonal world X and the set of facets located on a bisecting line between p_k and another site p_j , $j \neq k$. The size w_k of the first set is not greater than $|X|$, the number of facets of X . Thus $\sum_{k=1}^n w_k \leq n|X| = O(n)$. Denote by b_k the size of the second set. It is well known that $\sum_{k=1}^n b_k = O(n)$, in fact, $\sum_{k=1}^n b_k \leq 6n$. Indeed, from [9, p. 347], [61, pp. 173-5] we know that the number of edges in the Voronoi diagram is at most $3n$, and hence, since each edge

is counted twice (it is shared by two cells), we have $\sum_{k=1}^n b_k \leq 6n$. (In [9] it is assumed that the sites are in general position. However, if this is not true, then a small perturbation of them to a general position configuration actually enlarges the number of facets as explained in [61]. Hence $\sum_{k=1}^n b_k$ is bounded above by the number of edges in a general position configuration, which is bounded above by $3n$, as said before.) Therefore $\sum_{k=1}^n e_k = \sum_{k=1}^n w_k + \sum_{k=1}^n b_k \leq (6 + |X|)n = O(n)$ and the total number of nodes in the algorithm tree of the diagram is bounded above by $1 + \sum_{k=1}^n (2e_k - 1) = 1 + (11 + 2|X|)n = O(n)$. \square

Lemma 11.7. *Let ρ_k be the number of rays shot in the computation of the cell of the site p_k . Then*

$$\sum_{k=1}^n \rho_k \leq (|X| + 7)n. \tag{11.3}$$

Proof. The number ρ_k of shot rays is the sum of intermediate rays and the 3 initial rays. From the last paragraph of the proof of Lemma 11.5 we know that the first term is at most $e_k - 2$ (see (11.2)). Thus $\rho_k \leq e_k - 2 + 3 = e_k + 1$. Hence $\sum_{k=1}^n \rho_k \leq n + \sum_{k=1}^n e_k$. The proof of Lemma 11.6 implies that $\sum_{k=1}^n e_k \leq (|X| + 6)n$. We conclude that $\sum_{k=1}^n \rho_k \leq (|X| + 7)n$. \square

Lemma 11.8. *The number of calculations needed to find the endpoint in some given direction, using Method 5.1, is bounded by a linear expression of n .*

Proof. As in previous lemmas, one can build the algorithm tree for Method 5.1 (see also Figure 6). Each node is a place where it is checked whether the temporary endpoint y is in the cell (using distance comparisons). If yes, then the algorithm terminates, and if not, then y is further gets closer to the given site $p = p_k$. The obtained tree is linear. Whenever a distance comparison is made with some site $a = p_j, j \neq k$ (or even with p itself) and it is found that $d(y, p) \leq d(y, a)$, then there is no need to consider this site in later distance comparisons since the previous inequality means that y is in the halfspace of p (with respect to a) and because y always remains on the same ray and gets closer to p , it remains in this halfspace, i.e., also later temporary endpoints y will satisfy $d(y, p) \leq d(y, a)$. However, even if $d(a, p) < d(a, y)$ then a should not be considered anymore, since this case implies that y will be moved to the intersection between its ray and the bisecting line between p and a , and so in the next iterations it will satisfy $d(y, p) \leq d(y, a)$.

It follows that the total number of distance comparisons is not greater than n . A simple way to perform the above operation of not considering a given site anymore is to go over the array of sites by incrementing an index starting from the first site. By doing this each site will be accessed exactly one time and when the index arrives at the end, the process will end. Hence the number of nodes is $O(n)$. Each calculation done in a given node is either an arithmetic operation, array manipulations, etc., i.e., it is $O(1)$, or it involves a distance comparison (each comparison is $O(1)$). Hence the total number of calculation is $O(n)$ and the assertion follows. \square

Lemma 11.9. *The time complexity for computing the cell of p_k is bounded above by $O(r_k e_k)$, where r_k is the maximum number of distance comparisons done along*

each shot ray (compared between all shot rays), and e_k is the number of edges of the cell.

Proof. Lemma 11.5 implies that the size of the algorithm tree restricted to the cell of p_k contains at most $2e_k - 1 = O(e_k)$ nodes. The calculations done in each node are either calculations done when a ray is shot (for computing its endpoint) or some $O(1)$ calculations, when there is no need to compute a new endpoint (since the considered endpoints are already known) and only arithmetic operations, array manipulations, etc., are done. When an endpoint is computed, some operations are done along the corresponding ray. These operations are either distance comparisons or some related $O(1)$ operations (arithmetic operations, etc.: see the proof of Lemma 11.8). Hence the number of operations is linear in the number of distance comparisons and hence the maximum number of these operations, compared between all the shot rays, is $O(r_k)$. The upper bound $O(r_k e_k)$ follows. \square

Lemma 11.10. *The time complexity, for the whole diagram, assuming Q processing units are involved (independently) and processor Q_i computes a set A_i of cells, is $\max\{\sum_{k \in A_i} O(r_k e_k) : i \in \{1, \dots, Q\}\}$.*

Proof. This is a simple consequence of Lemma 11.9 because the processing units do not interact with each other and the cumulative time for computing a set of cells is the sum of times for computing each cell separately. \square

Lemma 11.11. *The time complexity of the algorithm for the whole diagram, when one processing unit is involved, is bounded above by $O(n^2)$.*

Proof. By Lemma 11.6 the time complexity of the algorithm for cell k is bounded by $O(r_k e_k)$. Since $r_k \leq n$ and $\sum_{k=1}^n e_k = O(n)$ (see the proofs of Lemma 11.8 and Lemma 11.6 respectively), the bound $O(n^2)$ follows. Alternatively, one can obtain the same bound using these lemmas directly (without referring to their proofs) since the number of nodes in the algorithm tree of the whole diagram is $O(n)$ and the number of calculations done in each node is at most $O(n)$. \square

11.2. The correctness of the output of the algorithm.

Lemma 11.12. *Let $F = \{\theta_1, \theta_2\}$ be a subfacet of the simplex and let $p + T(\theta_i, p)\theta_i$, $i = 1, 2$ be the corresponding endpoints.*

- (a) *If both endpoints are on the same facet, then the only possible vertices corresponding to F are the endpoints.*
- (b) *If one endpoint is on one facet and the other is on another one, and both facets intersect at some vertex v of the cell, then the only possible vertices corresponding to F are the endpoints and v .*

Proof. We first prove Part (a). This part seems quite obvious, but it turns out that a complete proof taking into account all the details requires some work. For an illustration, see Figure 13. Let $T_i = T(\theta_i, p)\theta_i$, $i = 1, 2$. By assumption, both endpoints $p + T_i$, $i = 1, 2$ are on some facet \tilde{L} of the cell. The segment $[p + T_1, p + T_2]$ is contained in \tilde{L} since \tilde{L} is convex. Suppose by way of contradiction that v is a

vertex corresponding to F which is not one of the endpoints $p + T_1, p + T_2$. Then v is strictly in the cone generated by the endpoints, that is, $v = p + \lambda_1 T_1 + \lambda_2 T_2$ for some $\lambda_1, \lambda_2 \in (0, \infty)$. A simple calculation (similar to that of (11.1)) shows that the ray emanating from p in direction $v - p$ intersects the segment $[p + T_1, p + T_2]$ in exactly one point w . It must be that $w = v$, since the part of the ray beyond w is strictly outside the cell of p , the part of the ray prior to w is strictly inside the cell, and v is in the cell and it is a boundary point. As a result, $v \in [p + T_1, p + T_2] \subseteq \widetilde{L}$. Since v is a vertex of the cell, it must belong to another facet \widetilde{M} .

Let $v' \neq v$ be some point in \widetilde{M} . Then v' cannot be on the line L on which \widetilde{L} is located, since in this case $\widetilde{L} \cap \widetilde{M}$ will include a non-degenerate interval (the interval $[v, v']$), a contradiction to the fact that two different facets intersect at a point or do not intersect at all. In addition, v' cannot be in the half-plane generated by L in which p is located. Indeed, suppose to the contrary that this happens (see Figure 13). First note that v' is not on the ray emanating from v and passing via p because this means that $[v, v']$, but this is impossible because p is an interior point. Indeed, a well known fact [67, Theorem 6.1, p. 45] says that because the underlying subset (the Voronoi cell in our case) is convex and because p is in its interior and v belongs to it, the half open segment $[p, v)$ is contained in the interior of the cell. Thus v' is in the interior of the cell, a contradiction. Consider now the cone generated by the rays emanating from p and passing via v and v' . Denote $\theta_v = (v - p)/|v - p|$ and $\theta_{v'} = (v' - p)/|v' - p|$. Any ray ϕ between θ_v and $\theta_{v'}$ close enough to θ_v (i.e., its generating unit vector is close enough to θ_v) intersects the segment $[v', v) \subset \widetilde{M}$, and later it intersects \widetilde{L} as a simple calculation shows (using the fact that v is in the open segment $(p + T_1, p + T_2)$ and the assumption on v'). However, once a ray emanating from p intersects a facet of the cell, then this point is its endpoint, namely, its remaining part beyond the point of intersection is outside the cell. Hence the point of intersection of the ray of ϕ with \widetilde{L} is outside the cell, contradicting the fact that it is on \widetilde{L} and hence it is in the cell.

As a result, the only possibility for v' is to be in the other half-plane generated by L , a contradiction to the fact that any point in this half-space is outside the cell. This contradiction completes the proof of part (a).

Now consider Part (b). Let $\theta_3 = (v - p)/|v - p|$, and let $F_1 = \{\theta_1, \theta_3\}$ and $F_2 = \{\theta_2, \theta_3\}$. The possible vertices corresponding to F are the ones corresponding to F_1 and F_2 . Because v belongs to two different facets it follows that $p + T_i, i = 1, 3$ are on one facet, and $p + T_i, i = 2, 3$ are on another facet. By Part (a) the only possible vertices corresponding to F_1 and F_2 are their corresponding endpoints $p + T_i, i = 1, 2, 3$, i.e., the endpoints corresponding to F and the vertex v . \square

Lemma 11.13. *The stored points are vertices of the cell of p .*

Proof. This is evident, since each such a point u is inside the cell and it is the intersection of two edges of the cell (line 22 of Algorithm 1). \square

In the following lemmas we use the concept of a “prime subfacet”, namely a subfacet created by the algorithm at some stage but which has not been further

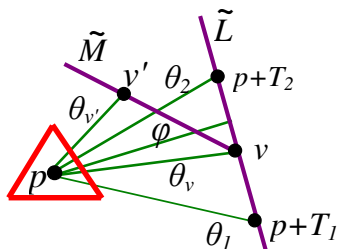


FIGURE 13. An illustration of one of the cases described in Lemma 11.12(a).

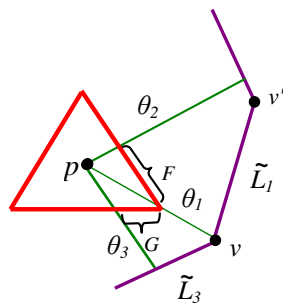


FIGURE 14. Illustration of Lemma 11.14.

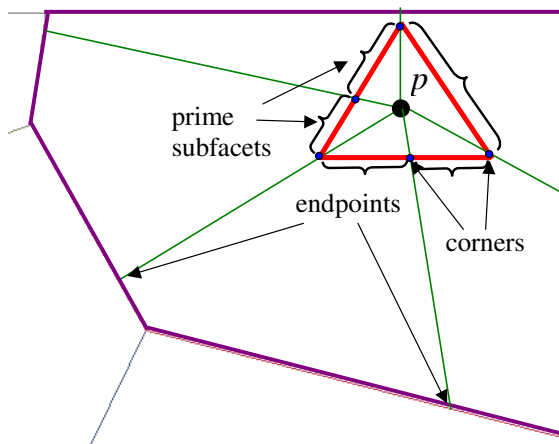


FIGURE 15. Prime subfacets and their rays.

divided after its creation. Because of Lemma 11.3 there are finitely many prime subfacets. Any two such subfacets either do not intersect or intersect at exactly one point (their corner), and their union is the simplex around p . See Figure 15 for an illustration.

Lemma 11.14. *Let v be a vertex of the cell and assume that it coincides with an endpoint corresponding to a corner of a prime subfacet F . Then v , as a vertex, is found and stored by the algorithm.*

Proof. The proof is not immediate as it may perhaps seem at first, since a vertex is found by the algorithm only after an intersection between two facets of the cell is detected, and so although v was found, as an endpoint, it is still not known that it is a vertex, and further calculations are needed in order to classify it as a vertex. Such a problematic situation mainly occurs at the routine of line 12 (the endpoints of a given subfacet are on the same facets), because even if one of the endpoints is

a vertex, it is not stored. Hence this vertex must be detected (and stored) when considering another subfacet.

Assume by way of contradiction that v , as a vertex, is not found. Let $p + T_1$ and $p + T_2$ be the endpoints corresponding to the corners of F . Let $\widetilde{L}_1, \widetilde{L}_2$ be the corresponding facets of the cell on which these endpoints are located. The facets $\widetilde{L}_i, i = 1, 2$ are located on corresponding lines L_1, L_2 . By assumption v coincides with one of the endpoints, say with $p + T_1$. See Figure 14.

Since $p + T_1$ corresponds to a corner of F , this corner is located on another prime subfacet G . Therefore v is also in the cone corresponding to G . Let $T_3 = T(\theta_3, p)\theta_3$. Let $p + T_3$ be the other endpoint corresponding to G . It is located on some facet \widetilde{L}_3 of the cell. Consider the lines L_1 and L_3 corresponding to \widetilde{L}_1 and \widetilde{L}_3 respectively. If they do not intersect, or intersect at a point outside the cone corresponding to G or inside the cone but outside the cell, then by the definition of the algorithm G must be divided, a contradiction (G is assumed to be prime). Note also that the equality $\widetilde{L}_3 = \widetilde{L}_1$ is impossible because it will imply that v is in the interior of the facet \widetilde{L}_1 and this cannot happen to a vertex. Hence $L_1 \neq L_3$ and it follows that L_1 and L_3 intersect at a point v_{13} which is in the cone and in the cell, i.e., a vertex.

A basic property of the polygonal boundary is that any facet of the cell intersects exactly two additional facets. In particular this is true for \widetilde{L}_1 : one intersection occurs at the vertex v and another one at another vertex v'' located on \widetilde{L}_1 in the direction (along \widetilde{L}_1) from v to $p + T_2$. Consider the line passing via p and v : it separates the plane into two halfplanes. One of them contains the ray θ_2 and actually \widetilde{L}_1 (and hence also v''). The other contains the ray θ_3 (and intersects \widetilde{L}_1 only at v) and hence also the facet \widetilde{L}_3 . Thus \widetilde{L}_3 cannot intersect \widetilde{L}_1 at the halfplane of v'' . Since we know that \widetilde{L}_3 intersects \widetilde{L}_1 this can only be at v . Hence $v_{13} = v$ but since v_{13} is a vertex, this means that v is found as a vertex when considering the subfacet G during the running time of the algorithm (line 21), a contradiction. \square

Lemma 11.15. *The algorithm finds all the vertices and edges of the cell.*

Proof. By Lemma 11.3 the algorithm terminates after a finite number of steps. Let $(F_j)_{j=1}^s$ be the finite list of all prime subfacets. Assume by way of contradiction that some vertex u is not found. Then u corresponds to some point located on some prime subfacet F of the simplex, since the ray in direction $u - p$ intersects the simplex at exactly one point, and each point on the simplex belongs to some prime subfacet.

Let $p + T_1$ and $p + T_2$ be the endpoints corresponding to the corners of F , and let $\widetilde{L}_1, \widetilde{L}_2$ be the corresponding facets of the cell on which these endpoints are located. The facets $\widetilde{L}_i, i = 1, 2$ are located on corresponding lines L_1, L_2 . Let B the matrix from (3.1).

Assume first that $\det(B) = 0$. Then it must be that $L_1 = L_2$, since otherwise L_1 and L_2 are parallel and hence F is divided into two subfacets (line 14), a contradiction. However, if $L_1 = L_2$, then $\widetilde{L}_1 = \widetilde{L}_2$, and hence, by Lemma 11.12(a), the only possible vertices corresponding to F are the endpoints $p + T_1, p + T_2$. In particular,

the missing vertex u coincides with one of these endpoints. But then, according to Lemma 11.14, the algorithm finds u as a vertex, a contradiction.

Assume now the case $\det(B) \neq 0$. Then $L_1 \neq L_2$. It must be that λ from (3.1) is nonnegative, since otherwise F is divided into two subfacets (line 26), a contradiction. The point of intersection between L_1 and L_2 is $v = p + \lambda_1 T_1 + \lambda_2 T_2$, and it must be in the cone corresponding to F and also in the cell of p , since otherwise F is divided into two subfacets (line 23). Hence v is a vertex corresponding to F and it is found by the algorithm at the stage when (3.1) is considered. If $v = u$, then the algorithm finds u when considering F , a contradiction. Hence $v \neq u$, and by Lemma 11.12(b) it must be that u coincides with one of the endpoints $p + T_1$ or $p + T_2$. But then, according to Lemma 11.14, the algorithm finds u as a vertex, a contradiction.

Therefore all the vertices of the cell are detected. As explained in Method 5.1 and Section 6, when a vertex is detected, also the edges which intersect at it are detected. Since all the possible vertices are found by the algorithm, then so are all the possible edges. \square

Proof of Theorem 9.1 with the exception of Part (e). This is a simple consequence of Lemmas 11.3, 11.9, 11.10, 11.11, 11.13, and 11.15. \square

11.3. Proof of Theorem 9.1 (e). In this subsection a proof of Theorem 9.1 is presented. The proof is based on several lemmas. Before formulating them, it is worth clarifying the expression “the sites are distributed independently according to the uniform distribution”. Here the probability space is X (the sampling space) together with the standard normalized Lebesgue measure which assigns to each region (a Lebesgue measurable subset of X) its area divided by the area of X . The location of each site is a random vector (from X to itself) and the probability for a site to be in some region of area σ is the ratio between σ and the area of X . All of these random vectors are assumed to be independent.

We start by formulating the following 3 known lemmas which will be used later. The proof of some of them is given for the sake of completeness.

Lemma 11.16. (An improvement of Stirling’s formula by Robbins [66])

Given a natural number ℓ , the following holds:

$$\ell! = \sqrt{2\pi\ell} \left(\frac{\ell}{e}\right)^\ell e^{r_\ell}, \quad (11.4)$$

where r_ℓ is a positive number satisfying $1/(12\ell + 1) < r_\ell < 1/(12\ell)$. In particular, $\ell! \geq \sqrt{2\pi\ell}(\ell/e)^\ell$.

Lemma 11.17. *Let $r \geq 1$. Then*

$$\left(1 - \frac{1}{r}\right)^r \leq e^{-1} \quad \text{and} \quad \left(1 + \frac{1}{r}\right)^r \leq e. \quad (11.5)$$

Proof. The assertion is obvious for $r = 1$. For all $r > 1$ let

$$f(r) := \left(1 - \frac{1}{r}\right)^r, \quad g(r) := \ln(f(r)) = r \ln\left(1 - \frac{1}{r}\right).$$

Then

$$g'(r) = \ln \left(1 - \frac{1}{r} \right) + \frac{r}{1 - \frac{1}{r}} \cdot \frac{1}{r^2} = \ln \left(1 - \frac{1}{r} \right) + \frac{1}{r-1}, \quad , g''(r) = \frac{1}{r-1} \left(\frac{1}{r} - \frac{1}{r-1} \right).$$

Therefore $g''(r) < 0$ for all $r > 1$ and hence g' is strictly decreasing on $(1, \infty)$. Since $\lim_{r \rightarrow \infty} g'(r) = 0$, elementary calculus shows that $g'(r) > 0$ for all $r > 1$. It follows that g is strictly increasing on $(1, \infty)$, and hence so is f . This implies the assertion because $\lim_{r \rightarrow \infty} f(r) = e^{-1}$. The second inequality in (11.5) can be proved in the same way. \square

Lemma 11.18. *Let $(\Omega, \mu, \mathcal{S})$ be a probability space where Ω is the sampling space, \mathcal{S} is the sigma algebra, and $\mu : \mathcal{S} \rightarrow [0, 1]$ is the probability function. Given events $E_1, \dots, E_\ell \subseteq \Omega$, we have*

$$\left(\sum_{i=1}^{\ell} \mu(E_i) \right) - (\ell - 1) \leq \mu(\cap_{i=1}^{\ell} E_i). \quad (11.6)$$

Proof. Let $E := \cap_{i=1}^{\ell} E_i$. Denote the complement of an event A by A' . Then

$$1 - \mu(E) = \mu(E') = \mu(\cup_{i=1}^{\ell} E'_i) \leq \sum_{i=1}^{\ell} \mu(E'_i) = \sum_{i=1}^{\ell} (1 - \mu(E_i)) \quad (11.7)$$

and the assertion follows. \square

The following 4 lemmas contain the core of the proof of Theorem 9.1(e).

Lemma 11.19. *Let $\alpha, \gamma \in \mathbb{N}$ be given. Assume that*

$$10 < m, \quad 3\alpha < \lfloor 0.2m \rfloor + 2, \quad \alpha\gamma < n. \quad (11.8)$$

Then the probability that at least $\gamma\alpha$ sites will be in a subset $V \subseteq X$ which consists of α small squares is not greater than

$$\frac{e^{4-0.8\alpha}}{\sqrt{\gamma\alpha}} \left(\frac{e}{\gamma} \right)^{\gamma\alpha} + \frac{e^{4+0.2\alpha}}{\sqrt{(\lfloor 0.2m \rfloor + 1)}} \left(\frac{e\alpha}{\lfloor 0.2m \rfloor + 1} \right)^{\lfloor 0.2m \rfloor + 1}. \quad (11.9)$$

If in addition $\sqrt{\alpha} \in \mathbb{N}$ and $\sqrt{\alpha} < \min\{m_1, m_2\}$, consider the set of all squares consisting of α small squares. Then the probability that at least $\gamma\alpha$ sites will be in at least one of these square is not greater than

$$n \left(\frac{e^{4-0.8\alpha}}{\sqrt{\gamma\alpha}} \left(\frac{e}{\gamma} \right)^{\gamma\alpha} + \frac{e^{4+0.2\alpha}}{\sqrt{(\lfloor 0.2m \rfloor + 1)}} \left(\frac{e\alpha}{\lfloor 0.2m \rfloor + 1} \right)^{\lfloor 0.2m \rfloor + 1} \right). \quad (11.10)$$

Proof. Let $j \in [\gamma\alpha, n]$ be a given natural number. The probability that some site a will be in the region V is α/m because the sites are distributed according to the uniform distribution and the ratio between the area of V to the area of X is α/m . Since there is independence between the sites, the probability of the event that some j different sites a_{i_1}, \dots, a_{i_j} will be in V and the other $n - j$ sites will be in $X \setminus V$ is $(\alpha/m)^j ((m - \alpha)/m)^{n-j}$. There are $\binom{n}{j}$ events of this kind and all of them are disjoint, so the probability of the event that exactly j sites are in V is

$\binom{n}{j}(\alpha/m)^j((m-\alpha)/m)^{n-j}$. The event E_V in which at least $\gamma\alpha$ sites are in V is the disjoint union of the events in which exactly j sites are in V , where j runs from $\gamma\alpha$ to n . We conclude that the probability of this event is

$$P(E_V) := \sum_{j=\gamma\alpha}^n \binom{n}{j} \left(\frac{\alpha}{m}\right)^j \left(\frac{m-\alpha}{m}\right)^{n-j}. \quad (11.11)$$

The goal now is to estimate $P(E_V)$ from above. First we observe that

$$n \leq m + 2\sqrt{m}. \quad (11.12)$$

Indeed, this follows from the facts that \sqrt{m} is an integer and $n = m + 2\sqrt{m}r + r^2 < m + 2\sqrt{m} + 1$ for some $r \in [0, 1)$. Let $j \in [\gamma\alpha, n] \cap \mathbb{N}$ be given. Either $j \leq 2\sqrt{m}$ or $j > 2\sqrt{m}$. In the first case

$$\begin{aligned} & \frac{(m+2\sqrt{m})(m+2\sqrt{m}-1)}{m} \dots \frac{(m+2\sqrt{m}-(j-1))}{m} \\ & \leq \frac{(m+2\sqrt{m})(m+2\sqrt{m}-1)}{m} \dots \frac{(m+1)}{m} \end{aligned} \quad (11.13)$$

In the second case (11.13) holds too because the following expression

$$\frac{m}{m} \cdot \frac{(m-1)}{m} \dots \frac{(m+2\sqrt{m}-(j-1))}{m} \quad (11.14)$$

appears as a factor in $((m+2\sqrt{m})/m)((m+2\sqrt{m}-1)/m) \dots (m+2\sqrt{m}-(j-1))/m$ in addition to $((m+2\sqrt{m})/m)((m+2\sqrt{m}-1)/m) \dots (m+1)/m$, and the factor (11.14) is a real number in $(0, 1]$ (this follows from $j \leq n$ and (11.12)). It follows from (11.12) and (11.13) that

$$\begin{aligned} \binom{n}{j} \left(\frac{\alpha}{m}\right)^j \left(\frac{m-\alpha}{m}\right)^{n-j} &= \frac{n(n-1) \dots (n-(j-1)) \alpha^j}{m^j j!} \left(1 - \frac{\alpha}{m}\right)^{(m/\alpha)\alpha(n-j)/m} \\ &\leq \frac{(m+2\sqrt{m})(m+2\sqrt{m}-1)}{m} \dots \frac{(m+1)}{m} \frac{\alpha^j}{j!} e^{\alpha(j-n)/m} \\ &\leq \left(1 + \frac{2}{\sqrt{m}}\right)^{4\sqrt{m}/2} \frac{\alpha^j}{j!} e^{-\alpha} e^{\alpha j/m} \leq e^4 \frac{\alpha^j}{j!} e^{-\alpha} e^{\alpha j/m}, \end{aligned} \quad (11.15)$$

where we used Lemma 11.17 in the first and third inequalities and $m \leq n$ in the second one. As long as $j \leq \lfloor 0.2m \rfloor$ we have $e^{-\alpha} e^{\alpha j/m} \leq e^{-0.8\alpha}$. For larger j we use the trivial estimate $j \leq n$, (11.12), and (11.8) (the fact that $m > 10$) to conclude that

$$e^{-\alpha} e^{\alpha j/m} \leq e^{\alpha(-1+1+(2/\sqrt{m}))} \leq e^{0.2\alpha}. \quad (11.16)$$

From (11.11),(11.8), (11.15),(11.16), and Lemma 11.16, it follows that

$$\begin{aligned}
 \sum_{j=\gamma\alpha}^n \binom{n}{j} \left(\frac{\alpha}{m}\right)^j \left(\frac{m-\alpha}{m}\right)^{n-j} &\leq \left(e^{4-0.8\alpha} \sum_{j=\gamma\alpha}^{\lfloor 0.2m \rfloor} \frac{\alpha^j}{j!}\right) + \left(e^{4+0.2\alpha} \sum_{j=\lfloor 0.2m \rfloor+1}^n \frac{\alpha^j}{j!}\right) \\
 &\leq e^{4-0.8\alpha} \frac{\alpha^{\gamma\alpha}}{(\gamma\alpha)!} \left(1 + \sum_{i=1}^{\infty} \frac{\alpha^i}{(\gamma\alpha+1)\dots(\gamma\alpha+i)}\right) + \\
 &\quad e^{4+0.2\alpha} \frac{\alpha^{\lfloor 0.2m \rfloor+1}}{(\lfloor 0.2m \rfloor+1)!} \left(1 + \sum_{i=1}^{\infty} \frac{\alpha^i}{(\lfloor 0.2m \rfloor+2)\dots(\lfloor 0.2m \rfloor+i+1)}\right) \\
 &\leq e^{4-0.8\alpha} \frac{\alpha^{\gamma\alpha}}{(\gamma\alpha)!} \left(1 + \sum_{i=1}^{\infty} \left(\frac{\alpha}{\gamma\alpha+1}\right)^i\right) + e^{4+0.2\alpha} \frac{\alpha^{\lfloor 0.2m \rfloor+1}}{(\lfloor 0.2m \rfloor+1)!} \left(1 + \sum_{i=1}^{\infty} \left(\frac{\alpha}{\lfloor 0.2m \rfloor+2}\right)^i\right) \\
 &= \frac{e^{4-0.8\alpha} \alpha^{\gamma\alpha}}{(\gamma\alpha)!} \left(\frac{1}{1-(1/(\gamma\alpha+1))\alpha}\right) + \frac{e^{4+0.2\alpha} \alpha^{\lfloor 0.2m \rfloor+1}}{(\lfloor 0.2m \rfloor+1)!} \left(\frac{1}{1-(1/(\lfloor 0.2m \rfloor+2))\alpha}\right) \\
 &\leq \frac{2e^{4-0.8\alpha} \alpha^{\gamma\alpha}}{\sqrt{2\pi\gamma\alpha}} \left(\frac{e}{\gamma\alpha}\right)^{\gamma\alpha} + \frac{2e^{4+0.2\alpha} \alpha^{\lfloor 0.2m \rfloor+1}}{\sqrt{2\pi(\lfloor 0.2m \rfloor+1)}} \left(\frac{e}{\lfloor 0.2m \rfloor+1}\right)^{\lfloor 0.2m \rfloor+1} \\
 &\leq \frac{e^{4-0.8\alpha}}{\sqrt{\gamma\alpha}} \left(\frac{e}{\gamma}\right)^{\gamma\alpha} + \frac{e^{4+0.2\alpha}}{\sqrt{(\lfloor 0.2m \rfloor+1)}} \left(\frac{e\alpha}{\lfloor 0.2m \rfloor+1}\right)^{\lfloor 0.2m \rfloor+1}
 \end{aligned}$$

where the first term in the right hand side of the first inequality is 0 if $\gamma\alpha > \lfloor 0.2m \rfloor$. This proves (11.9). It remains to show (11.10) under the assumption that $\sqrt{\alpha}$ is a natural number and $\sqrt{\alpha} < \min\{m_1, m_2\}$. Indeed, the number of all possible squares V_i consisting of α small squares is $(1+m_1-\sqrt{\alpha})(1+m_2-\sqrt{\alpha}) \leq m_1 m_2 = m \leq n$ (the left hand side is a natural number from the assumption on α). The probability that at least one of such V_i contains at least $\gamma\alpha$ sites is not greater than $\sum_i P(E_{V_i})$, which, from (11.9) is at most n times the expression in (11.9), as claimed. \square

Lemma 11.20. *In the notation and assumptions of Lemma 11.19, let E be the event in which at least one square which is composed of $\alpha \in \mathbb{N}$ small squares is empty of sites, where $\sqrt{\alpha}$ is an integer satisfying $\sqrt{\alpha} < \min\{m_1, m_2\}$. Then the probability of E is not greater than $ne^{-\alpha}$.*

Proof. Let V be a square which is composed of α small squares. The probability that some site a is not V is $(m-\alpha)/m$ because of the assumption of uniform distribution according to which the sites are distributed. Since there is independence between the sites, the probability that V is empty of sites is $(1-(1/m)\alpha)^n$. From Lemma 11.17 and the inequality $0 < \alpha < m \leq n$ we have

$$\left(1 - \frac{\alpha}{m}\right)^n = \left(1 - \frac{\alpha}{m}\right)^{(m/\alpha)\alpha n/m} \leq e^{-\alpha n/m} \leq e^{-\alpha}. \quad (11.17)$$

Consider the set of squares $V_i \subseteq X$ which are composed of α small squares. The probability of the event E is not greater than the sum over all indices i of the probabilities of the events that V_i is empty of sites. Since the number of squares

consisting of α small squares is at most $(1+m_1-\sqrt{\alpha})(1+m_2-\sqrt{\alpha}) \leq m_1m_2 = m \leq n$ (the left hand side is a natural number from the assumption on α), this probability is not greater than $ne^{-\alpha}$, as claimed. \square

Lemma 11.21. *In the setting of Lemma 11.19, let $\beta \in \mathbb{N}$ be given, and let E_1 be the event in which each square which is contained in X and composed of $\alpha_1 := (2\beta+1)^2$ small boxes contains at least one site. Let E_2 be the event in which each square which is contained in X and composed of $\alpha_2 := (1 + \lfloor 8\sqrt{2}(\beta+1.01) \rfloor)^2$ small boxes contains at most $\gamma\alpha_2 - 1$ sites. Let $E := E_1 \cap E_2$. Given $\gamma \in \mathbb{N}$, let F be the event in which at most $\gamma\alpha_2 - 1$ distance comparisons are made in the computation of each endpoint along each ray shot from each site p_k , $k \in K$ using Method 10.2. Then*

$$P(F) \geq P(E) \geq 1 - n \left(e^{-\alpha_1} + \frac{e^{4-0.8\alpha_2}}{\sqrt{\gamma\alpha_2}} \left(\frac{e}{\gamma} \right)^{\gamma\alpha_2} + \frac{e^{4+0.2\alpha_2}}{\sqrt{(\lfloor 0.2m \rfloor + 1)}} \left(\frac{e\alpha_2}{\lfloor 0.2m \rfloor + 1} \right)^{\lfloor 0.2m \rfloor + 1} \right). \quad (11.18)$$

Proof. The right inequality in (11.18) follows from Lemma 11.18, Lemma 11.20, and Lemma 11.19 which imply that

$$P(E) \geq P(E_1) + P(E_2) - 1 = 1 - (P(E'_1) + P(E'_2)) \geq 1 - n \left(e^{-\alpha_1} + \frac{e^{4-0.8\alpha_2}}{\sqrt{\gamma\alpha_2}} \left(\frac{e}{\gamma} \right)^{\gamma\alpha_2} + \frac{e^{4+0.2\alpha_2}}{\sqrt{(\lfloor 0.2m \rfloor + 1)}} \left(\frac{e\alpha_2}{\lfloor 0.2m \rfloor + 1} \right)^{\lfloor 0.2m \rfloor + 1} \right), \quad (11.19)$$

where G' is the complement of the event G . For showing $P(F) \geq P(E)$ is it sufficient to show that when E holds, then F holds, i.e., that $E \subseteq F$. The rest of the proof is devoted to showing this.

Indeed, consider an arbitrary site p_k , an arbitrary unit vector θ and let y be the candidate to be the first temporary endpoint along a ray in the direction of θ . According to Method 10.2 we have $y = p_k + 2\sqrt{2}(\beta+1.01)s\theta$ and there are a few possibilities. In the first, y is outside X . Then it is moved towards p_k so it will be on the boundary of X and then it satisfies $d(p_k, y) < 2\sqrt{2}(\beta+1.01)s$. Consider the integer square $S_I[y, 2\sqrt{2}(\beta+1.01)s]$. This square may not be contained entirely in X , but its intersection with X is contained in some integer square Q which is both contained in X and contains $(1 + \lfloor 4\sqrt{2}(\beta+1.01) \rfloor)^2$ small boxes: this is because from (9.8) the side lengths of X are much greater than $1 + \lfloor 4\sqrt{2}(\beta+1.01) \rfloor$ (for instance, if $X = [0, 300] \times [0, 300]$, $s = 1$, $\beta = 3$, and $y = (0.4, 50.2)$). Then y is in a small box whose indices are $(0, 50)$ and $2\sqrt{2}(\beta+1.01) \approx 11.34199$. Hence $S_I[y, 2\sqrt{2}(\beta+1.01)s]$ is contained in the integer square $Q := [0, 23] \times [50, 73]$ which is indeed contained in X and contains $(1 + \lfloor 4\sqrt{2}(\beta+1.01) \rfloor)^2 = 23^2$ small squares). By Lemma 10.5 it is sufficient to consider only the sites located in Q when performing distance comparisons along the ray in the given direction θ , because when going over all of these sites also all of the sites in $S_I[y, 2\sqrt{2}(\beta+1.01)s]$ will be considered.

In the second possibility y is in X and the integer square $S_I[y, \beta s]$ is contained in X . Because we assume that the event E_1 holds, it follows that $S_I[y, \beta s]$ contains a site, which, by Lemma 10.6, is closer to y than to p_k . As a result, y is the first temporary endpoint and according to Lemma 10.5 it is sufficient to consider for the distance comparisons along the considered ray only the sites located in $S_I[y, d(p_k, y)] = S_I[y, 2\sqrt{2}(\beta + 1.01)s]$. While this square may not be contained entirely in X , the dimensions of X (i.e., (9.8)) imply that $S_I[y, d(p_k, y)] \cap X$ is contained in some integer square Q which is both contained in X and contains $(1 + \lfloor 4\sqrt{2}(\beta + 1.01) \rfloor)^2$ small boxes. By Lemma 10.5 it is sufficient to consider only the sites located in Q when performing distance comparisons along the ray in the given direction θ , because when going over all of these sites also all of the sites in $S_I[y, 2\sqrt{2}(\beta + 1.01)s]$ will be considered.

In the third and last possibility y is in X and the integer square $S_I[y, \beta s]$ is not contained in X . According to Method 10.2 Step (4) we modify y to be $y := p_k + 4\sqrt{2}(\beta + 1.01)s\theta$. There are a few sub-possibilities now. In the first y is outside X . Then we move y towards p_k so it will be on the boundary of X . In particular, $d(y, p_k) < 4\sqrt{2}(\beta + 1.01)s$. By Lemma 10.5 it is sufficient to consider for the distance comparisons along the considered ray only the sites located in $S_I[y, d(y, p_k)]$. As usual, this square may not be contained entirely in X , but from (9.8) its intersection with X is contained in some integer square Q which is both contained in X and contains $(1 + \lfloor 8\sqrt{2}(\beta + 1.01) \rfloor)^2$ small boxes and as explained in previous paragraphs, by Lemma 10.5 it is sufficient to consider only the sites located in Q when performing distance comparisons along the ray in the given direction θ .

In the second and last sub-possibility y is inside X and hence we consider the integer square $S_I[y, 2\beta s]$, which at least quarter of it is contained in X (otherwise the side lengths of X would be less than $4\beta s$, a contradiction). This quarter of square is an integer square which contains $(2\beta + 1)^2$ small boxes. Since we assume that the event E_1 holds, this integer square has a site, which, by Lemma 10.6, is closer to y than to p_k . As a result, y is the first temporary endpoint and according to Lemma 10.5 it is sufficient to consider for the distance comparisons along the considered ray only the sites located in $S_I[y, d(y, p_k)] = S_I[y, 4\sqrt{2}(\beta + 1.01)s]$. The dimensions of X imply that the intersection of this square with X is contained in some integer square Q which is both contained in X and contains $(1 + \lfloor 8\sqrt{2}(\beta + 1.01) \rfloor)^2$ small boxes and it is sufficient to consider only the sites in Q for the distance comparisons.

Summarizing the above, in all possible cases, we need, for the distance comparisons along the considered ray in the given direction θ , to consider only sites located in some integer square Q . In all cases this square contains at most $\alpha := (1 + \lfloor 8\sqrt{2}(\beta + 1.01) \rfloor)^2$ small boxes. Since we assume that the event E_2 holds, it follows that there are at most $\gamma\alpha - 1$ sites in Q . Therefore, along the considered ray at most $\gamma\alpha - 1$ distance comparisons are made. Since p_k and θ where arbitrary, it follows that indeed the event E implies the event F , as claimed. \square

Lemma 11.22. *In the setting of Lemma 11.21, for all $k \in K$ and all rays shot during the computation of the cell of p_k using Method 10.2, one has that r_k , the maximum number of distance comparisons done along the rays, is not greater than*

$(1 + \lfloor 8\sqrt{2}(\beta + 1.01) \rfloor)^{2\gamma} - 1$ with probability which is at least the one described in (11.19). The total number of distance comparisons done in the computation of the whole diagram is not greater than $(\gamma(1 + \lfloor 8\sqrt{2}(\beta + 1.01) \rfloor)^2 - 1) \cdot 11n$ with probability which is also at least the one described in (11.19).

Proof. Lemma 11.21 and its proof show that $r_k \leq \gamma(1 + \lfloor 8\sqrt{2}(\beta + 1.01) \rfloor)^2 - 1$ with high probability which is described in (11.19). Denote by ρ_k the number of shot rays in the computation of the cell of p_k . The total number of distance comparisons done in the computation of all the cells is bounded by $\sum_{k=1}^n r_k \rho_k$. Since X is a rectangle, (11.3) shows that $\sum_{k=1}^n \rho_k \leq 11n$ and hence $\sum_{k=1}^n r_k \rho_k \leq (\gamma(1 + \lfloor 8\sqrt{2}(\beta + 1.01) \rfloor)^2 - 1) \cdot 11n$ as claimed. \square

It is now possible to prove Theorem 9.1(e).

Proof of Theorem 9.1(e). It is sufficient to use Lemma 11.22 with certain values of β and γ and to show that the parenthesis term in (11.19) is at most ϵ . Let $\gamma := 3$. As explained in Remark 9.2, both (9.1) and (9.2) do hold for all sufficiently large n . The relations (9.1)-(9.7) combined with straightforward calculations show that $(e/\gamma)^\gamma < 3/4$, that (11.8) holds with $\alpha := \alpha_2$, and that

$$\alpha_2/\alpha_1 \geq 4\sqrt{2}. \quad (11.20)$$

Therefore

$$(e/\gamma)^{\gamma\alpha_2} \leq (3/4)^{4\sqrt{2}\alpha_1} < 0.2^{\alpha_1} < e^{-\alpha_1}.$$

Because

$$\alpha_2 > (1 + \lfloor 8\sqrt{2} \rfloor)^2 = 23^2 = 529, \quad (11.21)$$

it follows that

$$\frac{e^{4-0.8\alpha_2}}{\sqrt{\gamma\alpha_2}} \left(\frac{e}{\gamma}\right)^{\gamma\alpha_2} < \frac{e^{-419}}{\sqrt{1587}} e^{-\alpha_1} < e^{-400} e^{-\alpha_1}.$$

Next we will prove that the second term in the parenthesis in (11.19) is smaller than $e^{-400} e^{-\alpha_1}$. Indeed, since $(e\alpha_2)/(\lfloor 0.2m \rfloor + 1) < e^{-1}$ by (9.2) and since (11.21) and (11.20) hold, it follows that

$$\begin{aligned} \frac{e^{4+0.2\alpha_2}}{\sqrt{(\lfloor 0.2m \rfloor + 1)}} \left(\frac{e\alpha_2}{\lfloor 0.2m \rfloor + 1}\right)^{\lfloor 0.2m \rfloor + 1} &< e^{4+0.2\alpha_2} e^{-0.2m} < e^{4+0.2 \cdot (-15\alpha_2)} \\ &< e^{4-2\alpha_2} e^{-\alpha_1} < e^{-400} e^{-\alpha_1}. \end{aligned}$$

Consequently, the above and (9.4) imply that

$$\begin{aligned} n \left(\frac{e^{4-0.8\alpha}}{\sqrt{\gamma\alpha}} \left(\frac{e}{\gamma}\right)^{\gamma\alpha} + \frac{e^{4+0.2\alpha}}{\sqrt{(\lfloor 0.2m \rfloor + 1)}} \left(\frac{e\alpha}{\lfloor 0.2m \rfloor + 1}\right)^{\lfloor 0.2m \rfloor + 1} \right) \\ < n(1 + 2e^{-400})e^{-\alpha_1} < \epsilon. \end{aligned}$$

Finally, by Lemma 11.22 and (9.7) the number of distance comparisons is bounded above by $(3\alpha_2 - 1) \cdot 11n = O(n \log(n/\epsilon))$. \square

12. CONCLUDING REMARKS

We would like to finish the paper with several remarks.

First, it should be emphasized again (see also Section 1) that this paper is theoretical. Hence no experimental data is given. Our paper is not unique regarding this: the computational geometry literature, in particular that one related to Voronoi diagrams, contains many papers discussing algorithms theoretically and without any experimental data. See e.g., [3, 6, 7, 13, 18, 20, 25, 26, 27, 41, 57, 58, 62, 65, 72, 77] for a rather partial list of such papers. Despite this, we want to say something about some practical issues, or, more precisely, about the current implementation we have.

Its actual behavior is somewhat strange: for a reason which is not currently well understood, the running time sometimes grows in a way which is a little bit greater than linear with respect to the input (number of sites) when one processing unit is involved. However, when several processing units are involved, then the running time $t(n)$ is better than linear with respect to the input (i.e., $t(\alpha n) < \alpha t(n)$ for all tested $\alpha \in \{1, 2, 3, \dots\}$; this does not contradict the obvious lower bound of $O(n)$). Perhaps (in both cases) this may be related to something in the memory management or some influence of the operating system.

Comparing to well-known implementations, our preliminary implementation performs quite good. For example, it runs faster than Qhull 2011.1 [12] when a Voronoi diagram of 10^6 sites is computed (a few seconds on a standard computer). However, it does not run faster than Triangle [74, 75]. Both Qhull and Triangle are veteran serial implementations (more than 17 years) which have adopted many enhancements over the years. Despite this, their behavior is worse than linear and their output is not always correct. In contrast, in our implementation only two people have been involved, for a not so long period, and only one of them has done the programming work. Many enhancements are waiting to be implemented. For instance, each vertex usually belongs to 3 cells and hence it is computed 3 times, while in Qhull/Triangle it is computed only once. In our implementation so far no incorrect output has been observed when double precision arithmetic was used.

A detailed description of experimental results, including comparisons to other known implementations such as CGAL [2] and Boost [1], and more details about implementation issues in various environments, will be discussed elsewhere.

The second remark is regarding Theorem 9.1(e). Although an $O(n \log(n/\epsilon))$ upper bound on the number of distance comparisons done in Method 10.2 for the computation of the whole diagram was given with probability $1 - \epsilon$, we believe that by a better analysis an $O(n)$ upper bound can be given (with the constant c inside the big O symbol which may depend on ϵ , say $c = 1/\epsilon$). This conjecture is supported by experimental tests. It seems that in order to obtain a linear upper bound one would need to improve the proof of Lemmas 11.19-11.20, since currently the upper bound on the union events mentioned there (the ones dealing with the set of all the squares composed of α small squares) is very coarse.

Third, we believe that it is possible to extend the methods described here to other settings, e.g., to compute Voronoi diagrams in higher dimensions and also to

compute other structures such as arrangements, certain manifolds, certain simplicial complexes, etc.

Finally, it is worth saying something about non-point sites. Algorithm 1 assumes that the sites are points. However, it is possible to consider sites of any form and to use the same algorithm, up to slight modifications. Indeed, suppose the sites P_k are compact sets located inside the world X . Each such a set can be approximated to any required precision by a finite subset of points contained in it. We then consider these points as P_k and compute the Voronoi cell of each of the points $p \in P_k$, namely $\{x \in X : d(x, p) \leq d(x, \cup_{j \neq k} P_j)\}$. The Voronoi cell of P_k is nothing but $\cup_{p \in P_k} \{x \in X : d(x, p) \leq d(x, \cup_{j \neq k} P_j)\}$. Now the array used to store the diagram becomes a 2-dimensional array, where the index p is added to it.

ACKNOWLEDGMENTS

Part of this work was done while the author was at IMPA (The National Institute of Pure and Applied Mathematics, Rio de Janeiro, Brazil) during 2011-2013 and was supported by a special postdoc fellowship (“Pós-doutorado de Excelência” postdoctoral scholarship). A certain preliminary part was done in 2010 while the author was at the Technion - Israel Institute of Technology. I want to thank several people regarding this this paper, among them Omri Azencot to whom I am indebted for implementing the algorithm so expertly and for helpful discussions, and Renjie Chen for helpful discussion regarding [21]. It is also an opportunity for me to thank the Gurwin Foundation and FAPESP.

REFERENCES

1. *Boost C++ Libraries, Generic Geometry Library (GGL)*, <http://www.boost.org/>.
2. *CGAL - Computational Geometry Algorithms Library*, <https://www.cgal.org>.
3. A. Aggarwal, B. Chazelle, L. J. Guibas, C. O’Dúnlaing, and C. K. Yap, *Parallel computational geometry*, *Algorithmica* **3** (1988), 293–327, preliminary version in FOCS 1985, pp. 468–477.
4. A. Aggarwal, L. J. Guibas, J. Saxe, and P. W. Shor, *A linear-time algorithm for computing the Voronoi diagram of a convex polygon*, *Discrete Comput. Geom.* **4** (1989), no. 6, 591–604, A preliminary version in STOC 1987, pp. 39-45.
5. O. Aichholzer, W. Aigner, F. Aurenhammer, T. Hackl, B. Jüttler, E. Pilgerstorfer, and M. Rabl, *Divide-and-conquer for Voronoi diagrams revisited*, *Proceedings of the 25th annual ACM Symposium on Computational Geometry (SoCG 2009)*, 2009, pp. 189–197.
6. P. D. Alevizos, J. Boissonnat, and M. Yvinec, *An optimal $o(n \log n)$ algorithm for contour reconstruction from rays*, *Proceedings of the Third Annual ACM Symposium on Computational Geometry (SoCG 1987)*, 1987, pp. 162–170.
7. N. M. Amato, M. T. Goodrich, and E. A. Ramos, *Parallel algorithms for higher-dimensional convex hulls*, *Proceedings of the 35th IEEE Symposium on Foundations of Computer Science (FOCS 1994)*, 683–694.
8. M. J. Atallah and D. Z. Chen, *Chapter 4 - deterministic parallel computational geometry*, *Handbook of Computational Geometry (J.-R. Sack and J. Urrutia, eds.)*, North-Holland, Amsterdam, 2000, pp. 155–200.
9. F. Aurenhammer, *Voronoi diagrams - a survey of a fundamental geometric data structure*, *ACM Computing Surveys* **3** (1991), 345–405.
10. F. Aurenhammer and R. Klein, *Voronoi diagrams*, *Handbook of computational geometry (J. Sack and G. Urrutia, Eds.)* (2000), 201–290.

11. C. B. Barber, D.P. Dobkin, and H.T. Huhdanpaa, *The Quickhull algorithm for convex hulls*, ACM Transactions on Mathematical Software **22** (1996), 469–483.
12. C. B. Barber and The-Geometry-Center, *Qhull (software)*, (2011), Copyright: 1993-2011. Web: <http://www.qhull.org>.
13. J. L. Bentley, B. W. Weide, and A. C. Yao, *Optimal expected-time algorithms for closest point problems*, ACM Trans. Math. Softw. **6** (1980), 563–580.
14. P. Berman and A. Lingas, *A nearly optimal parallel algorithm for the Voronoi diagram of a convex polygon*, Theoretical Computer Science **174** (1997), no. 1-2, 193–202.
15. G. E. Blelloch, J. C. Hardwick, G. L. Miller, and D. Talmor, *Design and implementation of a practical parallel Delaunay algorithm*, Algorithmica **24** (1999), 243–269.
16. K. Q. Brown, *Voronoi diagrams from convex hulls*, Inf. Process. Lett. **9** (1979), 223–228.
17. ———, *Geometric transforms for fast geometric algorithms*, Ph.D. thesis, Carnegie-Mellon University, Pittsburgh, 1980.
18. T. M. Chan and E. Y. Chen, *Optimal in-place and cache-oblivious algorithms for 3-d convex hulls and 2-d segment intersection*, Computational Geometry **43** (2010), 636–646, Special issue on SoCG 2009 (a preliminary version: SoCG 2009 pp. 80-89).
19. B. Chazelle and J. Matoušek, *Derandomizing an output-sensitive convex hull algorithm in three dimensions*, Computational Geometry **5** (1995), no. 1, 27–32.
20. ———, *Derandomizing an output-sensitive convex hull algorithm in three dimensions*, Computational Geometry **5** (1995), no. 1, 27–32.
21. R. Chen and C. Gotsman, *Localizing the delaunay triangulation and its parallel implementation*, Transactions on Computational Science XX (M. L. Gavrilova, C.J.K. Tan, and B. Kalantari, eds.), Lecture Notes in Computer Science, vol. 8110, Springer Berlin Heidelberg, 2013, Extended abstract in ISVD 2012, pp. 24–31, pp. 39–55 (English).
22. S.-W. Cheng, T. K. Dey, and J. R. Shewchuk, *Delaunay mesh generation*, CRC Press, Boca Raton, Florida, USA, 2012.
23. S. N. Chiu, D. Stoyan, W. S. Kendall, and J. Mecke, *Stochastic Geometry and its Applications*, third ed., John Wiley & Sons, Chichester, UK, 2013.
24. A. Chow, *Parallel algorithms for geometric problems*, Ph.D. thesis, University of Illinois, Urbana, 1980.
25. K. L. Clarkson, *Nearest neighbor queries in metric spaces*, Discrete and Computational Geometry **22** (1999), 63–93, preliminary version in STOC 1997, pp. 609–617.
26. K. L. Clarkson and P. W. Shor, *Applications of random sampling in computational geometry, II.*, Discrete Comput. Geom **4** (1989), no. 1, 387–421, Preliminaries versions in SoCG 1988, pp. 1–11, pp. 12–17.
27. R. Cole, M. T. Goodrich, and C. O’Dúnlaing, *A nearly optimal deterministic parallel Voronoi diagram algorithm*, Algorithmica **16** (1996), 569–617, a preliminary version in ICALP 1990, pp. 432–445.
28. R. Cole and C. K. Yap, *Shape from probing*, J. Algorithms **8** (1987), 19–38.
29. J. H. Conway and N. J. A. Sloane, *Sphere Packings, Lattices, and Groups*, third ed., Springer-Verlag, New York, 1999.
30. T. H. Cormen, C. E. Leiserson, R. L. Rivest, and C. Stein, *Introduction to algorithms*, second ed., MIT Press and McGraw-Hill, 2001.
31. N. Dadoun and D. G. Kirkpatrick, *Parallel construction of subdivision hierarchies*, J. Comput. Syst. Sci. **39** (1989), 153–165.
32. G. B. Dantzig, *Maximization of linear function of variables subject to linear inequalities*, Activity Analysis of Production and Allocation (T. C. Koopmans, ed.), Wiley & Chapman-Hall, New York-London, 1951, pp. 339–347.
33. ———, *Linear programming and extensions*, Princeton University Press, Princeton, N.J., 1963.

34. M. de Berg, O. Cheong, M. van Kreveld, and M. Overmars, *Computational geometry: Algorithms and applications*, third ed., Springer-Verlag, Berlin Heidelberg, 2008.
35. F. Dehne, A. Fabri, and A. Rau-Chaplin, *Scalable parallel computational geometry for coarse grained multicomputers*, Int. J. Comput. Geom. Appl. **06** (1996), no. 03, 379–400.
36. Q. Du, M. Emelianenko, and L. Ju, *Convergence of the Lloyd algorithm for computing centroidal Voronoi tessellations*, SIAM J. Numer. Anal. **44** (2006), 102–119.
37. Q. Du, V. Faber, and M. Gunzburger, *Centroidal Voronoi tessellations: applications and algorithms*, SIAM Rev. **41** (1999), no. 4, 637–676.
38. R. Dwyer, *Higher-dimensional Voronoi diagrams in linear expected time*, Discrete Comput. Geom. **6** (1991), no. 4, 343–367, A preliminary version in SoCG 1989, pp. 326–333.
39. H. Edelsbrunner, *Algorithms in combinatorial geometry*, Springer-Verlag, Berlin; New York, 1987.
40. D. J. Evans and I. Stojmenović, *On parallel computation of Voronoi diagrams*, Parallel Computing **12** (1989), 121–125.
41. S. Fortune, *A sweepline algorithm for Voronoi diagrams*, Algorithmica **2** (1987), 153–174, A preliminary version in SoCG 1986, pp. 313–322.
42. Y. Fragakis and E. Oñate, *Parallel Delaunay triangulation for particle finite element methods*, Commun. Numer. Meth. Engng. **24** (2008), 1009–1017.
43. C. Gold, *The Voronoi Web Site*, last updated: June 4, 2008, http://www.voronoi.com/wiki/index.php?title=Main_Page.
44. M. T. Goodrich, *Parallel algorithms in geometry*, Handbook of Discrete and Computational Geometry (J. E. Goodman and J. O’Rourke, eds.), Chapman and Hall/CRC Press, Boca Raton, FL, USA, 2nd ed., 2004, pp. 953–967.
45. M. T. Goodrich, C. O’Dúnlaing, and C. Yap, *Computing the Voronoi diagram of a set of line segments in parallel*, Algorithmica **9** (1993), 128–141, preliminary version in LNCS WADS 1989, pp. 12–23.
46. P. J. Green and R. Sibson, *Computing Dirichlet tessellations in the plane*, Comput. J. **21** (1977), 168–173.
47. P. M. Gruber and C. G. Lekkerkerker, *Geometry of Numbers*, second ed., North Holland, 1987.
48. L. Guibas, D. Knuth, and M. Sharir, *Randomized incremental construction of Delaunay and Voronoi diagrams*, Algorithmica **7** (1992), 381–413, A preliminary version in ICALP 1990, pp. 414–431.
49. L. J. Guibas and J. Stolfi, *Primitives for the manipulation of general subdivisions and the computation of Voronoi diagrams*, ACM Trans. Graph. **4** (1985), 74–123.
50. T. Hagerup and J. Katajainen, *Improved parallel bucketing algorithms for proximity problems*, Proceeding of the 26th Hawaii International Conference on System Sciences, vol. 2, 1993, pp. 318–327.
51. C. A. R. Hoare, *Quicksort*, The Computer Journal **5** (1962), 10–16.
52. G. J. Hwang, J. M. Arul, E. Lin, and C.-Y. Hung, *Design and multithreading implementation of the wave-front algorithm for constructing Voronoi diagrams*, Distributed and Parallel Computing, vol. 3719, 2005, pp. 257–266.
53. V. Klee, *On the complexity of d -dimensional Voronoi diagrams*, Arch. Math. **34** (1980), 75–80.
54. V. Klee and G. J. Minty, *How good is the simplex algorithm?*, Inequalities III (Proceedings of the Third Symposium on Inequalities held at the University of California, Los Angeles, Calif., September 1-9, 1969, dedicated to the memory of Theodore S. Motzkin) (O. Shisha, ed.), Academic Press, New York-London, 1972, pp. 159–175.
55. F. Lee and R. Jou, *Efficient parallel geometric algorithms on a mesh of trees*, Proceedings of the 33rd annual ACM Southeast Regional Conference, 1995, pp. 213–218.
56. C. Levcopoulos, J. Katajainen, and A. Lingas, *An optimal expected-time parallel algorithm for Voronoi diagrams*, SWAT 1988 (R. Karlsson and A. Lingas, eds.), Lecture Notes in Computer Science, vol. 318, Springer Berlin Heidelberg, 1988, pp. 190–198.

57. P. D. MacKenzie and Q. F. Stout, *Ultrafast expected time parallel algorithms*, Journal of Algorithms **26** (1998), no. 1, 1–33, preliminary version in SODA 1991, pp. 414–423.
58. H. Meyerhenke, *Constructing higher-order Voronoi diagrams in parallel*, EWCG 2005, pp. 123–126.
59. T. Ohya, M. Iri, and K. Murota, *Improvements of the incremental methods for the Voronoi diagram with computational comparison of various algorithms*, J. Operations Res. Soc. Japan **27** (1984), 306–337.
60. A. Okabe, B. Boots, K. Sugihara, and S. N. Chiu, *Spatial Tessellations: Concepts and Applications of Voronoi Diagrams*, second ed., Wiley Series in Probability and Statistics, John Wiley & Sons Ltd., Chichester, 2000, with a foreword by D. G. Kendall.
61. J. O'Rourke, *Computational geometry in C*, Cambridge University Press, New York, 1994.
62. S. Rajasekaran and S. Ramaswami, *Optimal parallel randomized algorithms for the Voronoi diagram of line segments in the plane*, Algorithmica **33** (2002), 436–460, a preliminary version in SoCG 1994, pp. 57–66.
63. S. Ramaswami, *Parallel randomized techniques for some fundamental geometric problems: A survey*, Parallel and Distributed Processing (J. Rolim, ed.), Lecture Notes in Computer Science, vol. 1388, Springer Berlin Heidelberg, 1998, pp. 400–407.
64. D. Reem, *An algorithm for computing Voronoi diagrams of general generators in general normed spaces*, Proceedings of the sixth International Symposium on Voronoi Diagrams in Science and Engineering (ISVD 2009), pp. 144–152.
65. J. H. Reif and S. Sen, *Optimal parallel randomized algorithms for three dimensional convex hulls and related problems*, SIAM J. Comput. **21** (1992), 466–485, Erratum: SIAM J. Comput. **23** (1994), 447–448.
66. H. Robbins, *A remark on Stirling's formula*, Amer. Math. Monthly **62** (1955), 26–29. MR 0069328 (16,1020e)
67. R. T. Rockafellar, *Convex Analysis*, Princeton University Press, Princeton, NJ, 1970.
68. T. Roos, *Maintaining Voronoi diagrams in parallel*, System Sciences, 1994. Proceedings of the Twenty-Seventh Hawaii International Conference on, vol. 2, Jan 1994, pp. 179–186.
69. O. Schwarzkopf, *Parallel computation of discrete Voronoi diagrams*, LNCS **349** (1989), 193–204, (Proc. of STACS 1989).
70. S. Sen, *Random sampling techniques for efficient parallel algorithms in computational geometry*, Ph.D. thesis, Computer Science Department, Duke University, 1989.
71. O. Setter, M. Sharir, and D. Halperin, *Constructing two-dimensional Voronoi diagrams via divide-and-conquer of envelopes in space*, Transactions on Computational Science **IX** (2010), 1–27, a preliminary version in ISVD 2009, pp. 43–52.
72. M. I. Shamos and D. Hoey, *Closest-point problems*, Proceedings of the 16th Annual IEEE Symposium on Foundations of Computer Science (FOCS 1975), 1975, pp. 151–162.
73. M. Sharir and P. Agarwal, *Davenport-Schinzel sequences and their geometric applications*, Cambridge University Press, Cambridge ;: New York, 1995.
74. J. R. Shewchuk, *Triangle: Engineering a 2D Quality Mesh Generator and Delaunay Triangulator*, Applied Computational Geometry: Towards Geometric Engineering (Ming C. Lin and Dinesh Manocha, eds.), Lecture Notes in Computer Science, vol. 1148, Springer-Verlag, 1996, From the First ACM Workshop on Applied Computational Geometry, pp. 203–222.
75. ———, *Delaunay refinement algorithms for triangular mesh generation*, Comput. Geom. **22** (2002), 21–74.
76. D. A. Spielman and S.-H. Teng, *Smoothed analysis: Why the simplex algorithm usually takes polynomial time*, Journal of the ACM **51** (2004), 385–463, A preliminary version in STOC 2001, pp. 296–305.
77. D. A. Spielman, S.-H. Teng, and A. Üngör, *Parallel Delaunay refinement: Algorithms and analyses*, International Journal of Computational Geometry and Applications **17** (2007), 1–30.

78. C. Treftz and J. Szakas, *Parallel algorithms to find the Voronoi diagram and the order-k Voronoi diagram*, Proc. of the International Parallel and Distributed Processing Symposium (IPDPS 2003).
79. B. C. Vemuri, R. Varadarajan, and N. Mayya, *An efficient expected time parallel algorithm for Voronoi construction*, Proceedings of SPAA 1992, pp. 392–401.

INSTITUTO DE CIÊNCIAS MATEMÁTICAS E DE COMPUTAÇÃO (ICMC), UNIVERSITY OF SÃO PAULO, SÃO CARLOS, AVENIDA TRABALHADOR SÃO-CARLENSE, 400 - CENTRO, CEP: 13566-590, SÃO CARLOS, SP, BRAZIL.

E-mail address: `dream@icmc.usp.br`